Ab initio determination of structural stability in fcc-based transition-metal alloys

C. Wolverton
Department of Physics, University of California, Berkeley, California 94720
and Materials Science Division, Lawrence Berkeley Laboratory, Berkeley, California 94720

G. Ceder
Department of Materials Science, Massachusetts Institute of Technology, Cambridge, Massachusetts 02139

D. de Fontaine
Department of Materials Science and Mineral Engineering, University of California, Berkeley, California 94720
and Materials Science Division, Lawrence Berkeley Laboratory, Berkeley, California 94720

H. Dreyssé
Laboratoire de Physique du Solide, Université de Nancy, Vandoeuvre-les-Nancy, France
(Received 30 October 1992; revised manuscript received 9 February 1993)

A cluster expansion is used to determine the energy of substitutionally disordered alloys as a function of configuration. The expansion is exact in the sense that the basis functions are complete and orthonormal. The coefficients, effective cluster interactions (ECI's), are computed directly from their definition by means of the method of direct configurational averaging, which is described in detail in the context of a tight-binding linear muffin-tin orbital (TB-LMTO) Hamiltonian. The alloy Hamiltonian is constructed from a combination of the pure-element TB-LMTO Hamiltonians, the hopping integrals between unlike pairs of atoms (simply given by the geometric mean of the pure-element integrals), and the potentials of the alloy, which are computed consistent with the condition that each configurationally averaged atom of the alloy be neutral. This scheme of self-consistency is tested against the results of fully self-consistent LMTO calculations on ordered compounds. The ECI's are computed on the fcc lattice for six alloy systems: Rh-Ti, Rh-V, Pd-Ti, Pd-V, Pt-Ti, and Pt-V. It is shown how the ECI's may be used in conjunction with properties of the energy expansion to exactly solve for the ground-state superstructures of fcc. This ground-state search is contingent upon minimizing the configurational energy subject to a number of geometric constraints. A large number of these constraints are formulated using group-theoretic means on the (13–14)-point clusters of the fcc lattice. The use of this large number of constraints makes possible the inclusion of fourth-nearest-neighbor pair ECI's as well as multiplet ECI's in the ground-state search. Both these types of interactions are shown to be essential towards obtaining a convergent energy expansion. In all six alloy systems, agreement between the theoretically predicted ground states and the experimental evidence of fcc superstructures is excellent: in no case is an unambiguously experimentally determined fcc-based phase missing from the results of the ground-state search.

I. INTRODUCTION

The study of phase stability in transition-metal alloys is of considerable technological interest. Any theoretical study of phase stability must begin with reliable, highly accurate expressions for the energy and entropy as a function of alloy composition (c) and temperature (T). Over the past few years, it has become possible to combine *ab initio* quantum-mechanical electronic band-structure calculations for alloy energetics with statistical-mechanics models for the entropy to obtain a free energy, $F=F(c,T)$, without the use of adjustable or experimentally determined parameters. The free energies between differing configurations may be compared, and the c-T phase diagram computed. Most of these studies involve transposing the alloy problem onto an "Ising-like" model where each atom of the alloy is assigned to (but not necessarily confined to) a site of an ideal lattice.

Within this Ising-like model of an alloy, Sanchez, Ducastelle, and Gratias (SDG) proved[1] that any function of configuration may be exactly expanded in terms of quantities based on clusters of lattice sites containing progressively greater number of points. Thus, these clusters of lattice sites are the fundamental building blocks of this sort of configurational description. Of course, the energetics of a given alloy will be affected not only by substitutional rearrangements of atoms on a fixed lattice, but also by topological or displacive variations. However, in many cases (particularly when the size mismatch between alloy constituents is small) the substitutional aspects of the problem dominate, and thus the entropy is limited to a configurational part and the energetics restricted to atoms sitting on the lattice sites.

Thus, for a given lattice, this Ising model provides the free energy for a given configuration, as a function of c and T. However, it is not possible, in practice, to exam-

0163-1829/93/48(2)/726(22)/$06.00

ine each of the possible configurations of N atoms, as this number grows exponentially with N. Therefore, in many phase diagram calculations, one tries to find the ground states, i.e., the minimum energy $T=0$ K states as a function of c, and then uses only these ground states in computing the phase diagram. Typically, these ground states are not derived, but either assumed or simply taken from the experimental phase diagram; however, these approaches are not predictive in nature, and in many cases detract from the spirit on the *ab initio* calculations used. In addition, most alloys of technological use are multicomponent, and experimental data may be sparse for these systems, or nonexistent. Thus, what is needed is a rigorous way of *deriving* the lowest-energy configurations on a given lattice for a specified alloy system. This paper addresses precisely this problem.

The energy of a binary alloy being a function of configuration (with respect to substitutional variations) may be expanded via the SDG formalism. Although the expansion is rigorous in principle by virtue of the fact that the basis functions used are orthonormal and complete in the space of the 2^N possible configurations, the cluster expansion is only useful in practice if it converges rapidly, so that it may be truncated at some stage with (hopefully) few important terms. Little is known analytically about the convergence, however numerical studies can shed some light on the situation by examining the behavior of the coefficients in the expansion. The coefficients are commonly referred to as effective cluster interactions (ECI's) or, perhaps more correctly, effective cluster parameters. The issue of convergence, which is critical to the use of the cluster expansion, if often neglected in studies involving the Ising-like alloy model. However, in this paper, we numerically investigate the convergence properties of the ECI's quite thoroughly. The ECI's are computed by means of the method of direct configurational averaging[2] (DCA), which is formulated here in terms of a tight-binding Hamiltonian. DCA is a method based in real space, not reciprocal space, and the idea behind the method is that the ECI's are computed as closely as possible from the exact definition of the SDG formalism.

Two distinct averaging schemes are currently used for defining the ECI's. In one scheme,[1] the ECI's are defined with respect to averaging over all configurations of the lattice, and are completely configuration independent, and hence concentration independent. In the other scheme,[3,4] the averaging is restricted to only those configurations consistent with a given concentration, thus leading to ECI's which are concentration dependent, but still configuration independent. The two schemes have been shown to be equivalent[4,5] (both numerically and analytically) and in the thermodynamic limit, the concentration independent ECI's are equal to the concentration dependent ones averaged at $c=\frac{1}{2}$.

The cluster expansion of alloy energetics in terms of concentration-independent ECI's is of interest for several reasons: (1) The problem of finding the minimum energy states of an alloy with respect to substitutional variations on a fixed lattice may be solved *exactly,* provided a rapidly convergent set of ECT's is known for that alloy system. As will be explained here, a rigorous search is prohibited by the use of concentration-dependent ECI's. (2) The energy expansion in terms of concentration-independent ECI's must contain multiplet (clusters with the number of points greater than two) interactions, otherwise the formation energies of a given alloy system will be completely symmetric about $c=\frac{1}{2}$, which is generally incorrect. Also, the cluster-variation method[6] (CVM), which is often used to calculate free energies of alloys within the Ising-like model, is most naturally formulated in terms of pair and multiplet correlations. Thus, the addition of the multiplet ECI's into a free-energy calculation poses no real problem in principle or in practice when using the CVM. (3) The ECI's provide an extremely convenient parametrization of the energy: Once the ECI's are known for a given alloy system, the energies of disordered and ordered states may be computed on an equal footing, and with relative ease. Thus, the ECI's coupled with a model for finite temperature effects (CVM, Monte Carlo,[7] etc.) provide thermodynamic data for ordered, partially ordered, and disordered states.

The primary focus of this paper is the calculation of the ECI's and subsequent use of the cluster expansion to rigorously derive the fcc ground-state structures in transition-metal alloys. While the ground states of a phase separating binary alloy are trivially defined (pure A and pure B), an ordering alloy may contain several intermediate compounds, and thus these ordering systems provide a much more critical test of the method of solving the ground-state problem proposed here. In transition metal alloys, d-band arguments[8] show that the most strongly ordered alloys will have an average bandfilling near the middle of the d band, or somewhere near five d electrons, whereas alloys with average bandfilling close to a completely empty or full d band will tend towards phase separation. Of course, exceptions have been found,[9] but in fact most transition-metal alloys with constituents on opposite ends of the transition-metal series do, in fact order, and in most cases, strongly so. Thus, we choose to study transition-metal alloys with one of the constituents near the beginning of the transition-metal series, and the other constituent near the end. Additionally, the transition metals with high d-electron count crystallize in the fcc structure so that it is reasonable to assume that alloys rich in these "late" transition metals will form superstructures of fcc, and thus predictions of the fcc ground-state search will be directly comparable to experiment. The six systems studied in this paper are those formed by alloying the fcc metals (late) Rh, Pd, and Pt with (early) Ti (hcp) and V (bcc): Rh-Ti, Rh-V, Pd-Ti, Pd-V, Pt-Ti, and Pt-V. Experimental evidence indicates that all these alloys are strongly ordered, and the Rh-, Pd-, and Pt-rich alloys tend to form fcc-based structures.

The paper is organized as follows: In Sec. II we define the Ising model used in the alloy description and review some of the properties of the cluster expansion. In particular, the energy expansion is explicitly demonstrated, and the exact definition of the coefficients in the expansion, the effective cluster interactions (ECI's), is given. Direct configurational averaging (DCA), a method for obtaining the ECI's straightforwardly from their

definition, is described in Sec. III. Section IV contains the formalism of the ground-state analysis, and shows how the use of the ECI's in conjunction with a judicious use of group theory provides for a rigorous ground-state determination. A brief description of the previous methods for ground-state analysis is given, as well as a discussion of the inadequacies of these methods in the transition-metal systems studied here. Results of the electronic band-structure calculations are given in Sec. V, in which checks on the self-consistency of the DCA are included. Additionally, the ECI's on the fcc lattice are computed for all six transition-metal alloys formed by combining Rh, Pd, and Pt with Ti and V. The fcc ground-state analysis is performed on all six alloys including pair and multiplet interactions which spatially extend up to the fourth-nearest-neighbor range, and comparison of the theoretical predictions is made with the available experimental evidence in Sec. VI. The final section, Sec. VII, contains a summary of the work and some general conclusions. The Appendix which follows contains details of the convergence properties of the ECI's and the cluster expansion.

II. CLUSTER EXPANSIONS

A. General expressions

To model a binary alloy, A_cB_{1-c}, consider a set of N atoms on a fixed lattice. The binary alloy is mapped onto an equivalent Ising-like problem by defining spin variables, σ_i, which are given the value $+1$ (-1) if an atom of type $A(B)$ is at site i. Thus, any configuration of the lattice may be represented by the N-dimensional vector, $\boldsymbol{\sigma}=(\sigma_1,\sigma_2,\ldots,\sigma_N)$. The inner product between any two functions of configuration $f(\boldsymbol{\sigma})$ and $g(\boldsymbol{\sigma})$ is defined as

$$\langle f(\boldsymbol{\sigma}),g(\boldsymbol{\sigma})\rangle=\frac{1}{2^N}\sum_{\{\sigma\}} f(\boldsymbol{\sigma})g(\boldsymbol{\sigma}) , \tag{2.1}$$

where the summation is over all configurations. Using this inner product, it can be shown[1] that any function of configuration may be expanded as

$$f(\boldsymbol{\sigma})=f_0+\sum_{\alpha} f_\alpha\sigma_\alpha , \tag{2.2}$$

where the summation is over all clusters α and where the configuration-independent term, f_0, has been extracted from the sum. The cluster functions $\sigma_\alpha(\boldsymbol{\sigma})$ are given by products of the spin variables over all sites, $p,p',\ldots,p''$, in the cluster α:

$$\sigma_\alpha=\sigma_p\sigma_{p'}\ldots\sigma_{p''} \tag{2.3}$$

and the generalized Fourier coefficients are given by

$$f_0=\langle 1,f(\boldsymbol{\sigma})\rangle , \tag{2.4}$$

$$f_\alpha=\langle \sigma_\alpha,f(\boldsymbol{\sigma})\rangle . \tag{2.5}$$

The expansion of Eq. (2.2) is *exact*. The cluster functions $\sigma_\alpha(\boldsymbol{\sigma})$ are complete and orthonormal with respect to the inner product operation of Eq. (2.1). However, the number of terms in the expansion is equivalent to the number of configurations, 2^N, thus, the practicality of this expansion in terms of cluster functions lies solely in its convergence properties. In one sense, the symmetry properties of the underlying lattice may enhance the convergence properties of the expansion: Because the inner product is defined by summing over all possible configurations of the lattice, the expansion coefficients maintain the symmetry of the lattice, and many [$\sim O(N)$] of the terms with equivalent clusters may be grouped together. Even so, there must be a sufficiently small number of inequivalent clusters with non-negligible generalized Fourier coefficients in order for the expansion to be a useful tool comparing the functional value of f for various configurations.

B. Configurational energy

One quantity which may be expanded in cluster functions is the configurational energy:

$$E(\boldsymbol{\sigma})=V_0+\sum_{\alpha} V_\alpha\sigma_\alpha , \tag{2.6}$$

where the generalized Fourier coefficients are now commonly referred to as effective cluster interactions (ECI's), and are given by expressions analogous to Eqs. (2.4) and (2.5):

$$V_0=\langle 1,E(\boldsymbol{\sigma})\rangle=\frac{1}{2^N}\sum_{\{\sigma\}} E(\boldsymbol{\sigma}) \tag{2.7}$$

and

$$V_\alpha=\langle \sigma_\alpha,E(\boldsymbol{\sigma})\rangle=\frac{1}{2^N}\sum_{\{\sigma\}} \sigma_\alpha E(\boldsymbol{\sigma}) . \tag{2.8}$$

To make Eq. (2.8) more transparent, consider the example of the effective pair interaction (EPI) between sites p and p': The cluster function σ_α takes the four values $+1$, $+1$, -1, and -1 depending on the four possible configurations of the pair, AA, BB, AB, and BA, respectively. Thus, the summation over all configurations in Eq. (2.8) may be split into two constituents: the sum over all of the configurations of the pair, and the sum over all the other sites, this latter quantity denoted by a primed sum. Then, Eq. (2.8) becomes

$$\begin{aligned} V_{pp'}&=\frac{1}{2^N}\left[\sum_{\sigma_p,\sigma_{p'}=-1}^{+1}\sigma_\alpha\left[\sum_{\{\sigma\}}{}' E(\boldsymbol{\sigma})\right]\right] \\ &=\frac{1}{2^2}\left[\frac{1}{2^{N-2}}\sum_{\{\sigma\}}{}'([E(\boldsymbol{\sigma})]_{(\sigma_p,\sigma_{p'})=(1,1)}+[E(\boldsymbol{\sigma})]_{(\sigma_p,\sigma_{p'})=(-1,-1)}-[E(\boldsymbol{\sigma})]_{(\sigma_p,\sigma_{p'})=(1,-1)}-[E(\boldsymbol{\sigma})]_{(\sigma_p,\sigma_{p'})=(-1,1)})\right] . \end{aligned} \tag{2.9}$$

This is usually written in a shorthand notation:

$$V_{pp'}=\tfrac{1}{4}[\{E_{AA}\}+\{E_{BB}\}-\{E_{AB}\}-\{E_{BA}\}] , \quad (2.10)$$

where the quantities $\{E_{IJ}\}$ are referred to as cluster energies (to be distinguished from effective cluster interactions) and are by definition, the average energy of all configurations with an I-J pair at sites p,p'. Note that the curly brackets of the cluster energies do not imply an ensemble or thermal average, but rather a simple, unweighted sum over configurations.

Expanding Eq. (2.8) for the cases of α representing a triplet of atoms at p,p',p'' gives

$$V_{pp'p''}=\frac{1}{8}[\{E_{AAA}\}+\{E_{ABB}\}-\{E_{AAB}\}-\{E_{ABA}\} -\{E_{BAA}\}-\{E_{BBB}\}+\{E_{BAB}\}+\{E_{BBA}\}] . \quad (2.11)$$

Higher-order clusters are given by generalizations of Eqs. (2.8)–(2.11).

In order to calculate these ECI's for a specific alloy system, then, the most straightforward method would involve explicitly computing the quantities in Eq. (2.10) or (2.11). However, this direct approach involves several difficulties: (1) There are 2^{N-2} terms in the summations of Eq. (2.10) and in the thermodynamic limit of $N\rightarrow\infty$, this clearly makes an exact calculation of all of these terms impossible. (2) Also, these summations involve *all* configurations of the lattice, and only an infinitesimally small number of these configurations actually possess some form of translational invariance. Thus, the standard techniques of band structure based on Bloch's theorem are not directly applicable to these completely disordered configurations. (3) The four terms in Eq. (2.10) involve energies of configurations which differ from one another by only one or two atoms. Therefore, an obvious practical difficulty of separately computing each term involves the determination of the small difference (the ECI) of large numbers (the energy of a given configuration). The method of direct configurational averaging (DCA), which is described below, overcomes all three of these obstacles, while maintaining the desirable property of calculating the ECI's from Eq. (2.10), which is known to be *exact*.

III. DIRECT CONFIGURATIONAL AVERAGING —FORMALISM

A. General energy expression

The derivation of the DCA equations will mainly pertain to the case of pair interactions, for simplicity. ECI's for larger clusters can be derived in an analogous manner, and where appropriate, the extension to multiplet interactions will be explicitly presented.

The total energy of a solid may generally be separated into two terms:[10] a one-electron band-structure contribution $E_{\rm BS}$ and an electrostatic term $E_{\rm ES}$, which includes several contributions. They are the Coulomb repulsion of the nuclei or ion cores and the correction for double counting the electron-electron interaction and the exchange and correlation energy in $E_{\rm BS}$. Thus, the cluster energies (and thus, the effective cluster interactions) of Eq. (2.10) must likewise include all of these contributions. It is usually assumed that, when taking the differences of cluster energies in the definitions of the ECI's,

$$V_{pp'}=\tfrac{1}{4}[\{E_{AA}\}+\{E_{BB}\}-\{E_{AB}\}-\{E_{BA}\}]\equiv\{\Delta_2 E_{pp'}\} , \quad (3.1)$$

the electrostatic terms cancel out, and hence, only the band-structure terms need be considered. This assumption has been shown to be valid in a number of alloy systems,[10–13] and will be tested against the results of total-energy calculations below. In Eq. (3.1), we have defined the difference operator Δ_2, which acts on any function of configuration $f(\sigma)$,

$$\Delta_2 f_{pp'}\equiv\tfrac{1}{4}[f_{AA}+f_{BB}-f_{AB}-f_{BA}] , \quad (3.2)$$

where f_{IJ} is the value of the function f with an I-J pair at sites p,p'. Note that the averaging over all sites except p and p' is not present in the definition of Δ_2. Also, for the purposes of this discussion, we will assume that the sites p,p' are implied by the use of Δ_2, and thus, these subscripts will be dropped. In general, the operator Δ_n represents the differences involved in an n-site ECI.

Therefore, what is required is the average over all sites, except p and p', of the $E_{\rm BS}$ contribution. The band-structure energy for a given configuration is, in general,

$$E_{\rm BS}(\sigma)=\int_{-\infty}^{E_F(\sigma)} En(E,\sigma)dE , \quad (3.3)$$

where $n(E,\sigma)$ is the total electronic density of states and $E_F(\sigma)$ is the Fermi level, both pertaining to a given configuration. Thus, in order to calculate the expressions for the ECI's, it is necessary to compute configurational averages of integrals, which is inconvenient in this case because the upper limit $E_F(\sigma)$ depends on the configuration. Following the derivation of Einstein and Schrieffer,[14] we reduce to a common Fermi level:

$$E_{\rm BS}(\sigma)=\int_{-\infty}^{E_F}(E-E_F)n(E,\sigma)dE+E_F\lambda , \quad (3.4)$$

where λ, the total charge of the system, is a constant (independent of configuration), and E_F is some (configurationally averaged) Fermi level. The computation of this averaged Fermi level is described in detail below. Certainly, Δ_2 acting on a constant function of configuration gives zero, thus

$$\Delta_2 E_{\rm BS}(\sigma)=\int_{-\infty}^{E_F}(E-E_F)\Delta_2 n(E,\sigma)dE , \quad (3.5)$$

and, therefore, in order to compute $V_{pp'}=\{\Delta_2 E(\sigma)\}$, we must evaluate $\Delta_2 n(E,\sigma)$ and thus $\Delta_2 E_{\rm BS}(\sigma)$ *and then average over all sites except p and p'*.

B. Expression for Δ_2 density of states

It is well known that the density of states may be related to the Green's function by

$$n(E,\sigma)=-\frac{1}{\pi}\,\mathrm{Im}\mathcal{G}(E,\sigma)$$
$$=-\frac{1}{\pi}\,\mathrm{Im}\frac{\partial}{\partial E}\ln\det(EI-\mathcal{H}(\sigma))\ . \tag{3.6}$$

Because the nature of the potentials at each point in the lattice depend on the type of the atom located there, the Hamiltonian is, of course, configuration dependent. Now, define $\mathcal{H}_{IJ}(\sigma')$ as the Hamiltonian corresponding to the pair *I-J* (*A* or *B*) located at p,p', with arbitrary σ' elsewhere. We write this quantity in block form

$$\mathcal{H}_{IJ}(\sigma')=\begin{bmatrix} H_{II} & H_{IJ} & H_{I0} \\ H_{JI} & H_{JJ} & H_{J0} \\ H_{0I} & H_{0J} & H_{00} \end{bmatrix}\ , \tag{3.7}$$

where H_{II} is the block of matrix elements which represent the interaction of atom I with itself, H_{IJ} represents the direct interaction of I with J, H_{00} pertains to the atoms of the medium surrounding the pair at p,p' interacting with each other, and H_{I0} pertain to the interactions of I with all the atoms in the medium. With N atoms in the system and ν orbitals on each site, H_{00} is of order $(N-2)\nu$ and H_{II} (or JJ or IJ) are of order ν.

We need to calculate

$$\Delta_2 n=-\frac{1}{\pi}\,\mathrm{Im}\frac{\partial}{\partial E}\Delta_2\ln\det(EI-\mathcal{H})\ . \tag{3.8}$$

One of the properties of a partitioned matrix, gives, in the present case

$$\det(EI-\mathcal{H}_{IJ})=\det G_{IJ}^{-1}\det(EI-H_{00})\ , \tag{3.9}$$

where G_{IJ} is the $2\nu\times2\nu$ top left block of the matrix $(EI-\mathcal{H}_{IJ})^{-1}$. Combining Eqs. (3.8) and (3.9) and using $\det G^{-1}=(\det G)^{-1}$ gives

$$\Delta_2\ln\det(EI-H)=\frac{1}{4}\ln\frac{\det(G_{AB})\det(G_{BA})}{\det(G_{AA})\det(G_{BB})}$$
$$=-\Delta_2\ln\det G\ . \tag{3.10}$$

It is seen that the huge determinant of order $(N-2)\nu$, $\det(EI-H_{00})$, cancels out.

C. Energy integration and orbital peeling

According to Eqs. (3.5), (3.8), and (3.10), it is required to calculate the integral

$$\Delta_2 E=\frac{1}{\pi}\,\mathrm{Im}\int_{-\infty}^{E_F}(E-E_F)\frac{\partial}{\partial E}\Delta_2\ln\det G(E)dE\ . \tag{3.11}$$

After integrating by parts, we arrive at the following expression for the effective pair interaction:

$$V_{pp'}=-\frac{1}{\pi}\left\{\mathrm{Im}\int_{-\infty}^{E_F}\Delta_2\ln\det G(E)dE\right\}\ . \tag{3.12}$$

The general expression for an n-site interaction may be written as

$$V_{p_1p_2\cdots p_n}=-\frac{1}{\pi}\frac{1}{2^n}\left\{\mathrm{Im}\int_{-\infty}^{E_F}\ln\left[\prod_{[\sigma_i]}^{(\mathrm{even})}\det G(E)_{[\sigma_i]}^{(\mathrm{even})}\right]\left[\prod_{[\sigma_i]}^{(\mathrm{odd})}\det G(E)_{[\sigma_i]}^{(\mathrm{odd})}\right]^{-1}dE\right\} \tag{3.13}$$

where the products $\prod^{(\mathrm{even})}$ and $\prod^{(\mathrm{odd})}$ are over the configurations of the n sites in the ECI, $[\sigma_i]$, with an even or odd number of B atoms, respectively. $G(E)_{[\sigma_i]}^{(\mathrm{even})}$ and $G(E)_{[\sigma_i]}^{(\mathrm{odd})}$ represent the top left $n\nu\times n\nu$ blocks of the matrix $(EI-\mathcal{H}_{[\sigma_i]})^{-1}$ for an even or odd number of B atoms in $[\sigma_i]$.

The $\det G$ can be calculated by the method of orbital peeling as described by Burke.[15] For short, denote by A any one of the four $(EI-\mathcal{H}_{IJ})$ matrices:

$$A=\begin{bmatrix} a_{11} & a_{12} & \cdots a_{1M} \\ a_{21} & a_{22} & \cdots a_{2M} \\ \vdots & \vdots & \ddots \\ a_{M1} & a_{M2} & \cdots a_{MM} \end{bmatrix}\begin{matrix} A_1 \\ A_2 \\ \vdots \\ A_M \end{matrix}\ . \tag{3.14}$$

Principal submatrices $A_1\ldots A_M$ have been indicated, where A_k is the matrix formed from A with the first $k-1$ rows and columns deleted. Typically, $M=N\nu$ where N is the total number of atomic sites, and ν is the number of orbitals per site. For any $1\le k\le M$, we have, with $D_k=\det A_k$, by the explicit formula for inverse matrices,

$$\frac{D_{k+1}}{D_k}=\bar{g}_k\ , \tag{3.15}$$

where $\bar{g}_k$ is the top left element of the matrix inverse to A_k. Therefore,

$$\prod_{k=1}^{M}\bar{g}_k=\frac{1}{D_M}\frac{D_M}{D_{M-1}}\frac{D_{M-1}}{D_{M-2}}\cdots\frac{D_2}{D_1}=\frac{1}{D_1}=\frac{1}{\det A}\ . \tag{3.16}$$

In Eq. (3.7), the H_{00} block is common to all *I-J* pairs. Hence, it is convenient to split up the product of Eq. (3.16) into

$$\left[\prod_{k=1}^{m}\bar{g}_k\right]\bar{g}_0,\quad\text{where }\bar{g}_0=\prod_{k=m+1}^{M}\bar{g}_k \tag{3.17}$$

in which $\bar{g}_0$ corresponds to H_{00}, and m is the order of $2\nu\times2\nu$ top left block of Eq. (3.7).

Hence, as in Eq. (3.10), the common factor $\bar{g}_0$ cancels, and we recover Eq. (3.10) with

$$\det G_{IJ}=\left[\prod_{k=1}^{m}\bar{g}_k\right] \tag{3.18}$$

and, therefore

$$\Delta_2 \ln \det G = \frac{1}{4} \sum_{k=1}^{m} \ln \left[\frac{\bar{g}_k^{AA} \bar{g}_k^{BB}}{\bar{g}_k^{AB} \bar{g}_k^{BA}} \right] . \tag{3.19}$$

Each $\bar{g}_k$ is the top left element of a partial Green's matrix. Therefore, Eq. (3.19), and hence, (3.12) can be calculated by summing over diagonal elements; off-diagonal Green's-function elements need never be calculated. However, each $\bar{g}_k^{IJ}$ must be calculated separately, for each of the 2ν cases. In a sense, the 2ν orbitals of the two atoms of the pair are peeled off one by one. The generalization of Eq. (3.19) for an n-site ECI is

$$\Delta_n \ln \det G = \frac{1}{2^n} \sum_{k=1}^{n\nu} \ln \left[\left[\prod_{\{\sigma_i\}}^{\text{even}} \bar{g}_k^{\{\sigma_i\}} \right] \left[\prod_{\{\sigma_i\}}^{\text{odd}} \bar{g}_k^{\{\sigma_i\}} \right]^{-1} \right] , \tag{3.20}$$

where the products are over configurations of the n-site cluster with an even or odd number of B atoms, and the quantities $\bar{g}_k^{\{\sigma_i\}}$ are the top left elements of the appropriate partial Green's matrix. In the general case, there are $n\nu$ orbitals, and for each orbital corresponds one diagonal Green's-function matrix element, which can be calculated by the recursion method, yielding an explicit continued fraction form. Thus, because of the large cancellations analytically derived and the method of peeling the orbitals of the clusters off one by one, the terms involved in the ECI's are not each calculated separately, which would lead to large subtractive errors, but rather, the differences are calculated directly, thus giving numerically stable results.

D. Evaluation of Green's-function elements by the recursion method

Any configuration of the alloy system may be described by the following tight-binding Hamiltonian:

$$H_{\text{alloy}} = \sum_{p,\lambda} |p,\lambda\rangle \varepsilon_p^{\lambda} \langle p,\lambda| + \sum_{p',p'',\mu,\nu}^{p' \neq p''} |p',\mu\rangle \beta_{p'p''}^{\mu\nu} \langle p'',\nu| , \tag{3.21}$$

where the Latin indices designate the lattice sites and the Greek indices label the orbitals. The ε's are the on-site energies and the β's are the hopping integrals. It is important to note that the fundamental idea of DCA is to compute the ECI's directly from expressions such as Eq. (2.10), hence, DCA is in no way confined to a tight-binding description. It is the physical transparency of this approach as well as the relative case of implementation which contribute to its appeal.

Within the context of this Hamiltonian, the recursion method[16] provides an efficient algorithm for obtaining diagonal elements of the Green's function, and hence, local densities of states. Given a starting vector, $|u_0\rangle$, one recursively generates a new set of vectors, $|u_i\rangle$, which can be constructed so as to be orthonormal, through the following set of operations:

$$\begin{aligned} b_0^2 &= \langle u_0 | u_0 \rangle , \\ a_i &= \langle u_i | H | u_i \rangle , \\ H|u_i\rangle &= a_i|u_i\rangle + b_{i+1}|u_{i+1}\rangle + b_i|u_{i-1}\rangle . \end{aligned} \tag{3.22}$$

Thus, the recursion coefficients a_i and b_i are the diagonal and off-diagonal elements of the Hamiltonian matrix defined by its new basis, in tridiagonalized form. The method also yields an explicit continued fraction form for the diagonal elements of the Green's function:

$$\langle u_0 | G | u_0 \rangle = \cfrac{b_0^2}{a_1 + E - \cfrac{b_1^2}{a_2 + E - \cfrac{b_2^2}{a_3 + E - \cdots}}} . \tag{3.23}$$

Of course, the algorithm must be stopped at some point, and thus, a terminator must be applied to the continued fraction. The choice of terminator for a given alloy system has been studied elsewhere,[17] and it is generally found that for transition-metal alloys, the effective cluster interactions are relatively insensitive to the choice of the terminator used. Thus, for these purposes, a quadratic one may be used.

The recursion method is well suited for computation of the Green's-function elements necessary in the definition of the ECI's. Also, because one operates exclusively in real space, the configurations of the alloy system studied need not be constrained by any symmetries (e.g., they need not be periodic).

IV. GROUND-STATE ANALYSIS—FORMALISM

The Ising-like energy expansion of Eq. (2.6) provides a convenient description of the energy of substitutional variations in configuration on a fixed lattice, provided a rapidly convergent set of ECI's are known for the particular alloy being studied. The Ising-like model, under favorable circumstances, may be solved exactly for the ground states which correspond to any given interactions. Of course, the solution will only give the lowest energy superstructures of the lattice for which the ECI's are computed. Thus, in this paper, we will only be examining the lowest-energy superstructures of the fcc lattice; however, the ground-state search has also been applied in three dimensions to the bcc (Refs. 18–20) and hcp (Refs. 21–25) lattices. Reviews of the ground-state problem may be found in Ducastelle[26] and Inden and Pitsch.[27]

The ground-state problem on the fcc lattice has been studied in detail. Kanamori derived the fcc ground states with first- and second-nearest-neighbor (NN) pair interactions,[18] as did Richards and Cahn,[28] and subsequently, Allen and Cahn.[29] The effect of multiplet interactions within the second-NN range was treated by Sanchez and de Fontaine,[30] who solved the ground-state problem including all clusters within the fcc tetrahedron octahedron. Sanchez and de Fontaine showed how the formulation of the cluster-variation method may be used to systematically derive the constraints of a given ground-state

problem. In total, it was found that 17 different structure types can be stabilized with all interactions in the tetrahedron-octahedron approximation. Several experimentally observed structures can only be stabilized with longer-ranged interactions. Unfortunately, the ground-state problem beyond the second-NN environment becomes quickly intractable. Using the method of geometrical inequalities Kanamori and Kakehasi[31] obtained many new structures by including third- and fourth-NN pair interactions in their analysis, however, their study did not exhaust all possible structures and did not allow for the presence of multibody interactions.

As shown here and also previously,[5,32,33] incorporation of interactions with a spatial extent of the fourth NN is sometimes essential to obtain a convergent energy expansion, and hence, the correct ground states. It is also essential to retain multiplet interactions in the energy expansion. The previous global fcc ground-state studies are then not generally applicable as they are obtained with a much more limited set of interactions. Recently, Lu *et al.*[34] used a simple enumeration technique to search for the ground states of several alloy systems in the presence of multibody interactions and pairs up to the fourth NN. The method of Lu *et al.* also incorporates an explicit volume dependence in the interactions, an effect not considered in this paper. However, such an enumeration method is incomplete in that any structure with a unit cell that extends outside some prescribed arrangement of $N_{\max}$ lattice sites ($N_{\max}=16$ in Ref. 34) would be missed. Of course, this limit, $N_{\max}$, could be increased if the system under study were suspected of possessing ground states with large unit cells, however, this would certainly result in a nontrivial increase in computer time (while a lower bound[35] on the number of distinct fcc-based structures with unit cells up to and including $N_{\max}=16$ is 69,639, a modest increase of four atoms per unit cell to $N_{\max}=20$ brings the number of structures to 528,873) and seriously limits the predictive capability of such a theory. In this paper we present an exact ground-state search for real transition-metal alloy systems on the fcc lattice, including pair and multiplet interactions which spatially extend to the fourth NN. The search is exact in the sense that with the interactions given, no other ground states may exist, irrespective of the size of the unit cell.

At $T=0$, the stable structure is that one that minimizes the energy [Eq. (2.6)]. Define the orbit of a cluster $\alpha,\Omega_L(\alpha)$, as the ensemble of all clusters that are related to α by a symmetry operation of the lattice (L). All clusters in an orbit have the same effective interaction V_α. Applying the lattice space-group symmetry to Eq. (2.6), we can thus write the energy as

$$E=V_0+\sum_{\Omega_L(\alpha)}^{\Omega_L(\alpha_M)}{}' V_\alpha N_\alpha \overline{\sigma_\alpha} \ . \tag{4.1}$$

The primed sum indicates that the empty cluster is not included. α_M indicates the maximal cluster which is kept in the expansion. N_α is the number of clusters in the orbit $\Omega_L(\alpha)$ and $\overline{\sigma_\alpha}$ is the *average* of the cluster spins in the orbit of α:

$$\overline{\sigma_\alpha}=\frac{1}{N_\alpha}\sum_{\alpha_i\in\Omega_L(\alpha)}\sigma_{\alpha_i} \ . \tag{4.2}$$

One should not confuse $\overline{\sigma_\alpha}$, which is a spatial average, with $\langle\sigma_\alpha\rangle$, which corresponds to the usual thermal average. We will refer to $\overline{\sigma_\alpha}$ as an orbit average. The fact that we define all orbits with respect to the symmetry of the lattice (L) does *not* mean that the structures we find from the ground-state search need to have this symmetry. In Eq. (4.1) we have simply grouped together variables that have the same effective cluster interaction. Dividing Eq. (4.1) by N, the number of lattice sites, gives us the energy per site:

$$e=\frac{V_0}{N}+\sum_{\Omega_L(\alpha)}^{\Omega_L(\alpha_M)}{}' V_\alpha m_\alpha \overline{\sigma_\alpha} \ , \tag{4.3}$$

where m_α is now the number of clusters of type α per lattice site. The term V_0/N can be omitted for the purpose of a ground-state analysis as it does not depend on the occupation of the lattice.

The orbit averages are constrained by the fact that they have to describe a physical state of ordering on the lattice. This is most easily expressed by requiring that all possible configurations on the maximal cluster in our expansion (α_M) occur with a relative probability between 0 and 1. The same condition is then automatically satisfied for the probability distribution on subclusters of α_M. Let $\rho(\boldsymbol{\sigma})$ be the probability distribution function for the configurations $\boldsymbol{\sigma}$ on the lattice. Since $\rho(\boldsymbol{\sigma})$ is, by definition, a function of the configuration, it can be formulated as an orthogonal expansion [like in Eq. (2.2)]:

$$\rho(\boldsymbol{\sigma})=\sum_\beta\langle\rho(\boldsymbol{\sigma}),\sigma_\beta\rangle\sigma_\beta(\boldsymbol{\sigma})=\frac{1}{2^N}\sum_\beta\langle\sigma_\beta\rangle\sigma_\beta(\boldsymbol{\sigma}) \ . \tag{4.4}$$

The reduced probability distribution ρ_α gives the probabilities for configurations (J) on the finite cluster α and can be obtained from $\rho(\boldsymbol{\sigma})$ as a partial trace:

$$\rho_\alpha(J)=\operatorname*{Tr}_{N-(\alpha)}\rho(\boldsymbol{\sigma})=\frac{1}{2^{n_\alpha}}\sum_{\beta\subseteq\alpha}\langle\sigma_\beta\rangle\sigma_\beta(J) \ . \tag{4.5}$$

Taking the orbit average on both sides of Eq. (4.5), one obtains

$$\overline{\rho_\alpha}(J)=\frac{1}{2^{n_\alpha}}\sum_{\beta\subseteq\alpha}\overline{\sigma_\beta}\sigma_\beta(J) \ , \tag{4.6}$$

since at $T=0$, $\langle\overline{\sigma_\beta}\rangle=\overline{\sigma_\beta}$. The average $\overline{\sigma_\beta}$ displays the symmetry of the lattice so that several of the subcluster correlation functions in Eq. (4.6) will be in the same orbit. It may thus be convenient to rewrite the expression for $\overline{\rho_\alpha}$ as

$$\overline{\rho_\alpha}(J)=\frac{1}{2^{n_\alpha}}\sum_{\Omega_L(\beta)\subseteq\alpha}\overline{\sigma_\beta}\sum_{\gamma\in\Omega_L(\beta),\gamma\in\alpha}\sigma_\gamma(J) \ . \tag{4.7}$$

The first summation is performed over all orbits that contain a subcluster of α. The second includes all subclusters of α in a given orbit and can be computed for a given configuration J on α:

$$\nu^J_{\alpha\beta}=\sum_{\gamma\in\Omega_L(\beta),\gamma\in\alpha}\sigma_\gamma(J)\ . \tag{4.8}$$

The matrix $\nu^J_{\alpha\beta}$ sometimes referred to as the v matrix, is used in the cluster-variation method to formulate the entropy in terms of the correlation functions.[36]

All function values of $\rho_\alpha(J)$ have to lie between 0 and 1. We can formulate this condition explicitly by evaluating Eq. (4.7) for all configurations J. Denote the probability to find configuration J on the clusters in the orbit of α as $\overline{X^J_\alpha}$:

$$\overline{X^J_\alpha}=\frac{1}{2^{n_\alpha}}\sum_{\Omega_L(\beta)\subseteq\alpha}\overline{\sigma_\beta}\nu^J_{\alpha\beta}\ , \tag{4.9}$$

The constraints on the orbit averages can be expressed as

$$0\le\overline{X^J_\alpha}=\frac{1}{2^{n_\alpha}}\sum_{\Omega_L(\beta)\subseteq\alpha}\overline{\sigma_\beta}\nu^J_{\alpha\beta}\ ,\quad\forall J \tag{4.10a}$$

and

$$\overline{X^J_\alpha}=\frac{1}{2^{n_\alpha}}\sum_{\Omega_L(\beta)\subseteq\alpha}\overline{\sigma_\beta}\nu^J_{\alpha\beta}\le 1,\quad\forall J\ . \tag{4.10b}$$

In addition, the normalization condition has to be imposed:

$$\sum_J\overline{X^J_\alpha}=1\ . \tag{4.11}$$

Note that Eq. (4.10a) together with Eq. (4.11) imply Eq. (4.10b), since a sum of positive terms can only equal 1 if each term is smaller than or equal to 1. In addition, Eq. (4.11) can be shown to be satisfied by the construction of Eq. (4.9).

The ground-state problem can thus be formulated as follows: Minimize the objective function (4.3) under constraints (4.10a) on the maximal cluster α_M. Since both objective function and constraints are linear in the orbit averages, the problem can be solved by linear programming.[37] Note that the ground-state problem becomes inherently nonlinear if concentration-dependent interactions are used. The concentration is linearly related to the point cluster function $\overline{\sigma_1}$, thus the use of concentration-dependent interactions makes the objective function (the energy) nonlinear because it has terms which are products of the cluster functions $\overline{\sigma_\alpha}$ and a function of $\overline{\sigma_1}$. Techniques are available to solve such problems; however, one is not guaranteed to find the global minimum of this nonlinear problem.

The minimum of Eq. (4.3) defines a set of orbit averages $\overline{\sigma_\alpha}$. When these averages uniquely describe a structure, the ground state is found. There still remains the problem of constructing the real structure from the orbit averages. In principle, the cluster functions contain the information necessary to describe the structure, however, because the information is averaged (through the orbit averages) the construction of the real structures from $\overline{\sigma_\alpha}$ is not always trivial. Formulating the constraints based on the probabilities of configurations of the maximal cluster being between zero and one provides a significant advantage in constructing the ground states: In addition to the orbit averages, the linear programming solution also gives all of the configurations of the maximal cluster which have a nonzero probability, the motives from which the structure is formed. Usually, the number of such configurations is quite small, and constructing the real-space structure from these motives is quite simple, and in the more complex cases can be systematically automated. The possibility also exists that no structure can be constructed with the set of orbit averages and is the result of the fact that we only constrain the orbit-averaged probability distribution function on α_M. Again, by considering the motives of the structure, it is possible in certain cases to *prove* that a particular solution corresponds to an inconstructible vertex. In some cases more than one structure corresponds to the orbit averages that minimize the energy. This ground-state degeneracy can be removed by considering a larger maximal cluster in the expansion [Eq. (4.3)] so that the orbit averages that distinguish the two structures are included in the ground-state analysis.

V. RESULTS: ELECTRONIC STRUCTURE CALCULATIONS

A. Total-energy LMTO calculations

Total-energy density-functional calculations were performed for the following five metals: Pt, Pd, Rh, V, and Ti, all in the fcc structure. The Kohn-Sham equations were solved in the local-density approximation[38,39] (LDA). The LDA was treated within the context of the method of linear muffin-tin orbitals[40] (LMTO) in the atomic sphere approximation (ASA) using the code of van Schilfgaarde.[41] Combined correction terms[42] to the ASA were not included. The computations were performed semirelativistically (including scalar relativistic corrections, i.e., excluding spin-orbit terms) and the exchange-correlation potential of von Barth and Hedin[43] was used. The basis set was composed of $l=0$, 1, and 2 orbitals. Convergence of the total energy with respect to k-point sampling was well within 0.1 mRy/atom, with the number of irreducible k points typically being 165. Self-consistent calculations were performed for each of the five pure elements at several values of the atomic volume, and the resulting total energies were fit to a third-order polynomial in volume. From this equation of state, the equilibrium lattice constant, Wigner-Seitz radius, bulk modulus, and pressure derivative of the bulk modulus were determined for each metal. The results of these computations are shown in Table I, along with the corresponding experimental results. The calculated equilibrium lattice constants are within $\sim 2\%$ of experimental numbers, but the LMTO-ASA calculations (without combined corrections) give a larger volume than experiment. The inclusion of combined correction terms in the LMTO Hamiltonian tends to decrease the equilibrium volumes, in most cases, below the experimental numbers, which is generally the case for LDA calculations. The bulk moduli are within 20% for the fcc metals Pt, Pd, and Rh. The discrepancy between calculated and experimental bulk moduli is slightly larger in the case of V and

TABLE I. Equilibrium ground-state properties of five transition metals in the fcc structure. The theoretical calculations are from an LMTO-ASA Hamiltonian, which is described in the text. Included are equilibrium lattice constant, Wigner-Seitz radius, bulk modulus, and pressure derivative of the bulk modulus. Comparison with experimental values is made when applicable.

Structure		a (Å)	R_{WS} (a.u.)	B_0 (Mbar)	B_0'
fcc Pt	Theory	4.02	2.97	2.90	5.2
	Expt.	3.92	2.89	2.78	
fcc Pd	Theory	3.95	2.92	2.09	5.4
	Expt.	3.89	2.87	1.81	
fcc Rh	Theory	3.88	2.86	2.78	3.7
	Expt.	3.80	2.81	2.71	
fcc V	Theory	3.79	2.80	2.04	3.4
bcc V	Expt.		2.82	1.62	
fcc Ti	Theory	4.07	3.00	1.27	3.6
hcp Ti	Expt.		3.05	1.05	

Ti. However, this is understandable, since the calculations are for the fcc structure whereas V and Ti crystallize in the bcc and hcp structures, respectively. Also, the effects of the anharmonic equation of state are seen clearly as the pressure derivatives of the bulk moduli deviate significantly from the harmonic value of -1. For the input to the alloy calculations to be described below, a linear dependence on alloy concentration was assumed for the alloy volume:

$$\Omega_{\text{alloy}}=c\Omega_A^0+(1-c)\Omega_B^0 , \tag{5.1}$$

where Ω_{alloy}, Ω_A^0, and Ω_B^0 are the alloy, pure A, and pure B volumes, respectively. Because the ECI's are averaged over all configurations (equivalent in the thermodynamic limit to an average at $c=\frac{1}{2}$), all of the pure-element computations to be used in the alloy calculations were repeated at the alloy volume given by Eq. (5.1) with $c=\frac{1}{2}$.

B. The alloy Hamiltonian

In light of the preceding formalism, the problem of computing ECI's for a given alloy system becomes dependent on the problem of constructing the alloy Hamiltonian. As shown above, the formalism is particularly convenient if the Hamiltonian is assumed to have a tight-binding form. The pure-element LMTO-ASA Hamiltonians were cast into the tight-binding (TB) representation in two-center form using the prescription of Andersen, Jepsen, and Sob.[44] Including the first-order terms of this formalism, the TB Hamiltonians have nonzero hopping integrals only between first- and second-NN pairs of atoms. In this study, the hopping integrals are assumed to depend only on the species at the site(s) in question, and the vector joining the two atoms:

$$\beta_{pp'}^{\mu\nu}=\beta_{I(p)\mu,J(p')\nu}(\mathbf{r}_I-\mathbf{r}_J) , \tag{5.2}$$

where $I(p)$ and $J(p')$ indicate the type of atoms ($I,J=A$ or B) at sites p and p'. In most alloy calculations, then, the hopping between two atoms of the same type is assumed to be independent of the local environment. Thus, the hopping integrals between like atoms, $\beta_{I\mu,I\nu}$, may be obtained from the pure elements. The hopping between unlike atoms is then given by the geometric mean of the appropriate pure element integrals:[45]

$$\beta_{I\mu,J\nu}=\sqrt{\beta_{I\mu,I\nu}\beta_{J\mu,J\nu}} . \tag{5.3}$$

This approximation can be derived from Hückel-type arguments, from free-electron theory, or from a multiple scattering (Korringa-Kohn-Rostoker) framework.[11]

In contrast to the hopping integrals, the on-site energies of the alloy may not be taken simply from the pure constituents. The effective potentials felt by each atom in an alloy are markedly different from those of the pure elements. Thus, these energy levels change upon alloying and a shift in the on-site energies is introduced:

$$\varepsilon_p^{\mu}=\varepsilon_{I(p)\mu}^0+\delta_{I(p)\mu} . \tag{5.4}$$

The superscript 0 is to represent the on-site energies of the pure elements and the quantity $\delta_{I(p)\mu}$ depends on the type of atom at site p as well as the orbital. For the express purpose of describing transition-metal alloys, where the primary resonances are in the d bands, we model the alloy by shifting the potentials of each of the orbitals of an atom by the same amount. Thus, $\delta_{I\mu}$ become independent of μ. In doing so, we neglect the importance of intra-atomic, interorbital charge transfers. The validity of this approximation has been tested and these tests will be described below. Also, because only *differences* of energies are involved in the definition of the ECI's, the only relevant quantity is the difference in the on-site energies of the alloy constituents. Thus, the quantities $\delta_{I\mu}$ are arbitrary for one of the alloy constituents, and may therefore be set equal to zero for $I=A$. We thus eliminate the I dependence of $\delta_{I\mu}$. The on-site energies of the B atoms of the alloy are all shifted with respect to those of the A atoms by the same amount, which we simply write, δ. The determination of this shift, δ, is of utmost importance in an accurate description of the alloy Hamiltonian.

The shift and Fermi level are both determined consistently with the condition that each of the configurationally averaged atoms be locally neutral: Using the recursion method, it is possible, as explained above, to obtain local densities of states (dos) on an atom of type I embedded in any configuration, σ. These dos are labeled $n_I^{\delta}(\sigma)$ (the δ superscript indicates that the dos are, of course, parametrized by the choice of δ). The procedure for obtaining δ and E_F is then as follows: (1) An arbitrary starting value of δ is chosen. (2) An A atom is surrounded by a configuration σ chosen completely at random and the local electronic occupation on this site is given by integrating the local dos. The Fermi level for this configuration is given by requiring

$$N_A(\sigma)=\int_{-\infty}^{E_F(\sigma)} n_A^{\delta}(\sigma,E)dE=N_A^0 , \tag{5.5}$$

where N_A^0 is the electronic occupation of an A atom in pure A, i.e., the locally neutral occupation. (3) Next, a B atom is embedded in the configuration σ. (It is not necessary that these two configurations be identical as these

occupations are to be configurationally averaged.) The occupation on the B atom is

$$N_B(\sigma)=\int_{-\infty}^{E_F(\sigma)} n_B^{\delta}(\sigma,E)dE \ , \tag{5.6}$$

where $E_F(\sigma)$ is the Fermi level determined by Eq. (5.5). For a given choice of δ, N_B will not in general be equal to N_B^0 as it must *on average* as guaranteed by global charge conservation. Steps (2) and (3) are repeated for a sufficient number of configurations (50 is used for this purpose), the number of which is dictated by convergence with respect to configurational averages and the accuracy required. (4) Simple configurational averages over these 50 passes are made, with these averages being denoted by curly brackets. Thus, of course $\{N_A\}=N_A^0$ is guaranteed because it is required for each configuration. However, if $\{N_B\}\neq N_B^0$, then the choice of δ is incompatible with configurationally averaged neutrality (CAN), and a new value of δ must be chosen, and the entire procedure is repeated starting from step (1). This process is continued until a value of δ is found which gives $\{N_B\}=N_B^0$, within some suitable threshold, which is typically 0.01 electrons. The configurationally averaged Fermi level to be used in the computation of the ECI's is then given by $\{E_F(\sigma)\}=E_F$. The resulting potentials are consistent with CAN. That is, for any given random configuration, each site is not neutral, but rather some small amount of negative and positive charge will be loaned to or borrowed from its neighbors. However, on average, this charge transfer from A to B atoms (and vice versa) is zero.

TABLE II. Coordinates and multiplicities of the effective cluster interactions on the fcc lattice. In order to maintain integer coordinates, the unit-cell size is taken to be $a=2$.

Cluster size	ECI	Coordinates	Multiplicity
Pairs	$V_{2,1}$	(000),(110)	6
	$V_{2,2}$	(000),(200)	3
	$V_{2,3}$	(000),(211)	12
	$V_{2,4}$	(000),(220)	6
	$V_{2,6}$	(000),(222)	4
Triplets	$V_{3,1}$	(000),(011),(110)	8
	$V_{3,2}$	(000),(110),(200)	12
	$V_{3,3}$	(000),(101),(211)	24
	$V_{3,4}$	(000),(101),(202)	6
	$V_{3,5}$	(000),(112),(220)	12
	$V_{3,6}$	(000),(121),(21−1)	8
	$V_{3,7}$	(000),(020),(200)	12
	$V_{3,8}$	(000),(112),(211)	24
	$V_{3,9}$	(000),(020),(112)	24
	$V_{3,10}$	(000),(220),(222)	24
	$V_{3,11}$	(000),(202),(220)	8
	$V_{3,12}$	(000),(110),(222)	24
	$V_{3,13}$	(000),(110),(112)	24
	$V_{3,14}$	(000),(110),(022)	48
Quadruplets	$V_{4,1}$	(000),(011),(101),(110)	2
	$V_{4,2}$	(000),(101),(110),(200)	12
	$V_{4,3}$	(000),(101),(202),(303)	6
	$V_{4,4}$	(000),(1−10),(110),(200)	3
	$V_{4,5}$	(000),(002),(020),(200)	24
	$V_{4,6}$	(000),(002),(110),(200)	24
	$V_{4,7}$	(000),(110),(112),(222)	12
	$V_{4,8}$	(000),(020),(202),(222)	6

C. Computation of the ECI's

Once the alloy Hamiltonian and average Fermi level are determined, the ECI's may be calculated using the formalism of Sec. III. ECI's were calculated for six transition-metal alloys: Rh-Ti, Pd-Ti, Pt-Ti, Rh-V, Pd-V, and Pt-V. Convergence of the interactions was checked with respect to the number of levels of recursion used in the computation of the Green's-function matrix elements. Ten levels of recursion were found to be sufficient and was used in all of the computations. The zebra technique[46] was used to construct the total system of lattice sites for each ECI. This recursion crystal contained between $N=1012$ and 1339 atoms, dependent upon the spa-

TABLE III. Effective cluster interactions for fcc Pd-V. The value of $\Sigma_{\text{conf}}/\sqrt{N_{\text{conf}}}$ gives a quantitative estimate of the error induced by considering only a finite number of configurations, N_{conf}, in the averaging process (see Appendix).

Cluster size	Effective cluster interaction (ECI)	V_α (meV/atom)	$\Sigma_{\text{conf}}/\sqrt{N_{\text{conf}}}$ (meV/atom)	N_{conf}
Pairs	$V_{2,1}$	+57.0	3.2	50
	$V_{2,2}$	−15.5	0.30	50
	$V_{2,3}$	+4.3	0.49	50
	$V_{2,4}$	+2.5	0.75	50
	$V_{2,6}$	+0.4	0.02	50
Triplets	$V_{3,1}$	+11.7	0.29	30
	$V_{3,2}$	+0.8	0.18	30
	$V_{3,3}$	−2.2	0.06	30
	$V_{3,4}$	+5.4	0.05	30
	$V_{3,5}$	a	a	15
	$V_{3,6}$	−0.1	0.05	15
	$V_{3,7}$	−0.4	0.04	15
	$V_{3,8}$	−0.3	0.02	15
	$V_{3,9}$	a	a	15
	$V_{3,10}$	a	a	15
	$V_{3,11}$	a	a	15
	$V_{3,12}$	a	a	15
	$V_{3,13}$	−0.1	0.04	15
	$V_{3,14}$	−0.2	0.05	15
Quadruplets	$V_{4,1}$	−1.5	0.004	20
	$V_{4,2}$	−0.5	0.01	20
	$V_{4,3}$	+0.2	0.003	20
	$V_{4,4}$	−0.5	0.01	20
	$V_{4,5}$	a	a	10
	$V_{4,6}$	a	a	10
	$V_{4,7}$	a	a	10
	$V_{4,8}$	a	a	10

[a]The calculations for these interactions gave values less than 0.1 meV.

tial extent of the interaction in question. These numbers correspond to five full shells of nearest neighbors and next-nearest neighbors surrounding the two-, three-, or four-point cluster of the ECI.

In order to obtain a good representation of the energy as a function of configuration through Eq. (4.3), it is necessary that no non-negligible terms in the expansion be omitted. In other words, all of the ECI's with values above some suitable threshold must be included. To this end, 27 ECI's have been calculated for all six systems, which represents the largest set of interactions used in any study of alloy energetics. The coordinates which serve to define the clusters are given in Table II, as are the multiplicities [defined in Eq. (4.3)]. The ECI's are labeled as $V_{n,m}$, where n is the number of sites in the cluster and m is simply a label of the type of cluster. In the case of pairs, m represents the mth NN spacing. The ECI's of Table II then include the first- through fourth- and sixth-NN pairs (these are all the pairs which are included in the standard 14-point fcc cube), 14 different triplet interactions and eight quadruplet interactions.

The ECI's for the Pd-V system and the five remaining systems are given in Tables III and IV, respectively. The convergence of the cluster expansion and the ECI's (with respect to configurational averaging) are both critically important in the utilization of the expansion, thus a detailed study of these properties is included here in an appendix. From the results therein, we establish with some confidence that the energy expression is well converged. In considering the results of Tables III and IV, several general statements may be made about the alloy systems: First, all of the NN pair interactions dominate, and all are strongly positive, indicative of ordering tendencies, which is experimentally observed in all these systems. Although the 2nd, 3rd, and 4th NN pairs are decaying, all of these interactions are significant. By the time the 6th NN pair is reached, the pair interactions have decayed practically to zero for all systems. It is also interesting to note that in each system, we have $V_{2,2}<0$ and $V_{2,3}>0$. In the Rh-based systems, the multiplet interactions are quite small, indicating that the formation energies of these systems should be sensibly symmetric about concentration 1/2. Thus, for instance, it is likely that the Rh_3V ground state is similar to that of RhV_3. In the Pd- and Pt-based alloys, the triplets are of varying importance; however, in the Pd-Ti system, the NN triplet $V_{3,1}$ (composed of three NN bonds), is quite large, almost

TABLE IV. Effective cluster interactions on the fcc lattice. Values are given for ECI's without multiplicity (see Table II).

		V_α (meV/atom) Alloy system				
Cluster size	ECI	Rh-Ti	Pd-Ti	Rh-V	Pt-Ti	Pt-V
Pairs	$V_{2,1}$	+59.3	+47.4	+48.8	+127.7	+90.1
	$V_{2,2}$	−3.5	−13.8	−9.5	−17.4	−17.3
	$V_{2,3}$	+9.9	+8.5	+7.9	+13.6	+5.2
	$V_{2,4}$	+0.2	+0.9	−0.4	+6.4	+4.4
	$V_{2,6}$	−0.3	a	a	+0.7	a
Triplets	$V_{3,1}$	+3.6	+19.6	+3.3	+8.7	+4.8
	$V_{3,2}$	+1.4	+0.8	+1.0	+1.3	+0.4
	$V_{3,3}$	+3.4	a	+1.1	+1.5	−1.3
	$V_{3,4}$	a	+5.9	+1.4	+10.0	+6.2
	$V_{3,5}$	a	a	a	a	a
	$V_{3,6}$	a	a	a	+0.2	+0.4
	$V_{3,7}$	−0.2	−0.2	−0.2	−0.9	a
	$V_{3,8}$	−0.2	+0.6	a	−0.2	−0.4
	$V_{3,9}$	a	a	a	a	+0.2
	$V_{3,10}$	a	a	a	a	a
	$V_{3,11}$	a	a	a	−0.1	a
	$V_{3,12}$	a	a	a	−0.2	−0.2
	$V_{3,13}$	a	+0.2	−0.1	−0.2	a
	$V_{3,14}$	−0.3	−0.3	−0.2	−0.7	−0.3
Quadruplets	$V_{4,1}$	−1.8	−4.2	−0.3	−2.9	−1.2
	$V_{4,2}$	−0.6	−1.0	−0.2	−1.1	−1.0
	$V_{4,3}$	a	+0.5	a	+0.8	+0.3
	$V_{4,4}$	−0.2	−1.2	a	−1.5	−0.8
	$V_{4,5}$	a	a	a	a	a
	$V_{4,6}$	a	a	a	a	a
	$V_{4,7}$	a	a	a	a	a
	$V_{4,8}$	a	a	a	a	a

[a]The calculations for these interactions gave values less than 0.1 meV.

half as large as $V_{2,1}$. Also, from these six alloy systems, it is clear that the triplet interactions, $V_{3,1-4}$, are consistently significant indicating that any study of transition-metal alloys should not neglect these interactions. The NN triangle and linear triplet, $V_{3,1}$ and $V_{3,4}$, are particularly large for several systems. These two ECI's have also been found to be important in other tight-binding calculations.[5] The other triplets are, for the most part, insignificant, although $V_{3,14}$ can be important especially when it is considered that the multiplicity for this cluster is 48: For example, although the Pt-Ti value is -0.7 meV for this interaction, it may contribute as much as 33 meV to the energy. In the ground-state analysis to be discussed below, this sort of energy difference can be crucial. The quadruplet interactions are also quite small, with the nearest-neighbor tetrahedron $V_{4,1}$ being the largest among them. Surprisingly, the linear four-body interaction $V_{4,3}$ is quite small (even in comparison with $V_{4,1}$) in all six systems.

D. Tests of self-consistency and configurationally averaged neutrality (CAN)

The potentials felt by the constituents of the alloy are calculated in accordance with the condition of CAN, as explained above. It is possible to compare this scheme of self-consistency based on CAN against fully self-consistent LMTO calculations on ordered compounds. As a first test, we compare the alloy potentials computed from the shifted pure-element on-site energies with those of a fully self-consistent LMTO calculation. As shown in Ref. 4, averaging over all configurations of a system is equivalent to averaging at $c=1/2$, in the thermodynamic limit, thus we choose an ordered compound with stoichiometry AB for the comparison, for example, the AuCu, or $L1_0$ structure.[47] (Although the $L1_0$ phase has tetragonal symmetry, the calculations were performed on an ideal fcc lattice, with $c/a=1$, so that these ordered structure calculations could be directly compared with the DCA results.) Table V shows such a comparison for the Pd-V and Pt-V systems. The difference in on-site energies is a relevant measure of the diagonal disorder of the system (the diagonal part of the Hamiltonian which is dependent on configuration). So, we define a diagonal disorder parameter:

$$\Delta_d^\mu=\varepsilon_A^\mu-\varepsilon_B^\mu-\delta\ , \tag{5.7}$$

where μ is the index corresponding to the angular momentum and crystal-field symmetry of the given on-site energy. The shift δ is calculated in the completely disordered state as explained above in the case of pure element TB-LMTO input. However, for the $L1_0$ calculation, the TB transformation is done on the LMTO Hamiltonian after self-consistency is achieved, thus there are no shifts of the potentials in this case. Additionally, another approximation made in the self-consistency of the DCA is that the hopping integrals are independent of the environment. The hopping between two A atoms, for example, is assumed to be the same in the pure element as in the alloy. The off-diagonal disorder (configuration-dependent, off-diagonal elements of the Hamiltonian) is therefore treated correctly [within Eq. (5.3)] in the DCA, but the magnitude of off-diagonal disorder is dictated by the pure-element integrals. In transition metals, the critical part of the off-diagonal elements of the Hamiltonian is in the d bands, as demonstrated by a wealth of calculations (Refs. 5, 8, 10, 48, and 49). Because the d-band width of an alloy is closely tied to the magnitude of the ddi ($i=\sigma,\pi,\delta$) hopping integrals, it is appropriate to define a qualitative estimate of the off-diagonal disorder in a given transition-metal system as the ratio of d-band widths of the two constituents of the alloy. Consequently, we define a d-band off-diagonal disorder parameter as

$$\Delta_{\rm od}=\frac{\beta_{dd\sigma}^{AA}}{\beta_{dd\sigma}^{BB}}\ , \tag{5.8}$$

where $\beta_{dd\sigma}^{II}$ is the $dd\sigma$ hopping integral for an I-I pair of atoms.

TABLE V. Comparison of diagonal disorder and off-diagonal disorder for two self-consistency schemes. In one case, TB-LMTO pure-element calculations are used as input, along with the self-consistency condition of configurationally averaged neutrality (CAN), and in the second case, the tight-binding Hamiltonian is from a fully self-consistent LMTO calculation of the $L1_0$ structure.

System			Pure elements/ CAN	Fully self-consistent $L1_0$ calculation
Pd-V	$\Delta_d^\mu=\varepsilon_{\rm Pd}-\varepsilon_{\rm V}-\delta$ (Ryd)	s:	-0.141	-0.155
		p:	-0.026	-0.067
		t_{2g}:	-0.268	-0.271
		e_g:	-0.266	-0.266
	δ (Ryd)		-0.040	
	$\Delta_{\rm od}=\beta_{dd\sigma({\rm Pd})}/\beta_{dd\sigma({\rm V})}$		0.89	0.90
Pt-V	$\Delta_d^\mu=\varepsilon_{\rm Pt}-\varepsilon_{\rm V}-\delta$ (Ryd)	s:	-0.369	-0.362
		p:	-0.067	-0.091
		t_{2g}:	-0.261	-0.266
		e_g:	-0.264	-0.269
	δ (Ryd)		$+0.016$	
	$\Delta_{\rm od}=\beta_{dd\sigma({\rm Pt})}/\beta_{dd\sigma({\rm V})}$		1.22	1.19

Table V shows the diagonal and off-diagonal disorder parameters for Pd-V and Pt-V, first within the self-consistency and CAN of the DCA, and second for a fully self-consistent LMTO calculation for the $L1_0$ compound which is subsequently transformed into the TB representation. The values of Δ_d^μ agree remarkably well in both systems for the t_{2g} and e_g on-site energies, the agreement being within 3 mRy for the Pd-V case and 5 mRy for Pt-V. These sorts of differences, O(mRy) are negligible when it is considered that the pure-element potentials are shifted by a considerably larger amount. (For a typical case, a 1 mRy shift of the potentials corresponds to a transfer of approximately 0.02 electrons, and changes typical ECI values by roughly 1%.) The s and p on-site energies are not quite as well represented in the DCA self-consistency, but this is quite possibly due to the more free-electron-like nature of these electrons. For

transition-metal alloys, where d-band resonances are paramount, these sorts of errors in s and p bands do not in most cases lead to significantly different energies. It is interesting to note that the s bands are represented better than the p bands and that in both systems, the CAN result gives a value of Δ_d^p, which is 25–40 mRy higher than the fully self-consistent result. This is presumably an artifact of the orbital-independent on-site energy shifts. Also, the off-diagonal disorder parameter is in excellent agreement with the fully self-consistent calculation. In the DCA, the hopping integrals are assumed to be independent of substitutional configuration changes in the local environment, thus Δ_{od} for the DCA is exactly that of the pure elements. In the $L1_0$ calculation, this ratio of hopping integrals differs only by approximately 3% or less. Thus, we see that the approximations made in the self-consistency of the DCA are on a firm physical footing, and agree quite well with fully self-consistent calculations.

Because Pd and Pt are isoelectronic, the magnitude of diagonal disorder in these two systems should be roughly equal, as diagonal disorder is driven mainly by electronic occupation. This is indeed the case for all of the on-site energies except the s band. The value of Δ_d^s is ~ 0.2 Ry smaller for the Pd-V alloy than for Pt-V, indicative of a significant deepening of the s band of Pt. The inclusion of the relativistic mass velocity and Darwin terms in the Hamiltonian has been shown[9] to be responsible for the s-band lowering in Pt, and these terms are included in the LMTO Hamiltonian (and consequently, in the TB-LMTO Hamiltonian). The deepening of the Pt s band significantly increases the ordering tendencies of several Pt-based alloys,[9] and is again demonstrated here: The Pt-V system has a much larger NN pair interaction (90 meV) than does Pd-V (57 meV), which indicates a much more strongly ordered system. The increase in ordering tendencies has been ascribed to either the increase in ionic bonding caused by increased transfer of electrons into the Pt s band,[50] or a stronger covalent bonding caused by the increase in s-d hybridization;[51] however, because we have, in this paper enforced CAN and ignored the electrostatic terms of the total energy, an increase in s-d hybridization seems to be the more likely cause. Thus, the s-band cohesion is a significant effect, especially important when considering transition metals of the 5d row.

Table V illustrates the differences in alloy Hamiltonians between the self-consistency and CAN of the DCA, and a fully self-consistent LMTO calculation. In Table VI, we see directly the effects of self-consistency *on the ECI's*. Table VI has two columns, one of which corresponds to the DCA calculation with CAN enforced, and one corresponds to the self-consistent $L1_0$ computation, which is subsequently transformed into the TB representation. In both cases, the TB Hamiltonians were used to compute several of the ECI's for the Pd-V system. In every case except the NN pair, the ECI's agree to within 1 meV for these two methods of self-consistency, and the discrepancy in all of the interactions is small enough to be simply the result of configurationally averaging over a small set of configurations. The quadruplet interactions are not effected even to 0.1 meV by the use of the fully self-consistent Hamiltonian. Also, the results of the ground-state analysis (see below) are not changed by using the second column of interactions in place of the first. Thus, as a result of Tables V and VI, it is clear that the self-consistency procedure outlined above for the DCA is clearly adequate, and is in excellent agreement with fully self-consistent results for the case of these transition-metal alloys.

VI. RESULTS: GROUND-STATE ANALYSIS

As shown in Sec. V and the Appendix, it is essential in fcc to retain pair interactions up to fourth-NN spacing and multiplet interactions in order to obtain a convergent energy expansion. To include both these types of interactions we have formulated the fcc ground-state problem

TABLE VI. Comparison of effective cluster interactions for fcc Pd-V computed with the two distinct self-consistency schemes of Table V.

Cluster size	Effective cluster interaction (ECI)	Pure elements/CAN V_α (meV/atom)	Fully self-consistent $L1_0$ calculation V_α (meV/atom)
Pairs	$V_{2,1}$	+57.0	+61.4
	$V_{2,2}$	−15.5	−16.0
	$V_{2,3}$	+4.3	+3.9
	$V_{2,4}$	+2.5	+3.4
Triplets	$V_{3,1}$	+11.7	+10.8
	$V_{3,2}$	+0.8	+0.6
	$V_{3,3}$	−2.2	−2.2
	$V_{3,4}$	+5.4	+5.5
Quadruplets	$V_{4,1}$	−1.5	−1.5
	$V_{4,2}$	−0.5	−0.5
	$V_{4,3}$	+0.2	+0.2
	$V_{4,4}$	−0.5	−0.5

with the 13- and 14-point clusters as maximal clusters (Fig. 1), an approximation which contains 742 distinct cluster orbits, including all pair interactions up to the 6th NN, except for $V_{2,5}$. The use of large maximal clusters makes possible the inclusion of more pair and multibody interactions in the ground-state analysis. The constraints [Eq. (4.10a)] were obtained with a computer code that uses group-theory concepts to systematically automate the computation of the coefficients $\nu^J_{\beta\alpha}$ from Eq. (4.8).[52] There are 554 constraints for the 14-point cluster and 288 for the 13-point cluster. Thus, in this (13–14)-point approximation, the ground-state problem is formulated in terms of a 742-dimensional space with 842 linear constraints imposed. The minimization of the energy was performed with a linear programming routine using the simplex algorithm.[37]

The ground-state equations (as a function of concentration) were solved for each of the six alloys systems: Rh-Ti, Rh-V, Pd-Ti, Pd-V, Pt-Ti, and Pt-V. The minimum energy solutions were found for each system, retaining 26 interactions of Table II in the cluster expansion. $V_{4,3}$, which is not a subcluster of the (13–14)-point clusters, was not included in the energy expansion. Most of the superstructures found in these ground-state analyses have been described elsewhere. These references, along with the Strukturbericht designation, the Pearson symbol, prototype, and space group are given in Table VII. In this paper, a structure will be referred to by its Strukturbericht designation when one exists. If there is none, then the prototype will be used, and, if there exists no experimentally observed prototype, an alternate labeling scheme will be used.

It is often necessary to give the energy of the ground states relative to some specified reference point. This reference is usually taken to be the concentration-weighted average of the pure-element energies, and the resulting energy difference is the formation energy. For a given structure s with a concentration of A atoms equal to c_A, the formation energy is given by

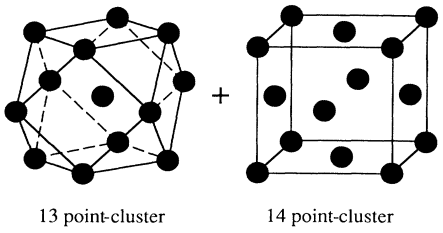

FIG. 1. The 13- and 14-point fcc clusters. In the ground-state searches, the probabilities of cluster configurations are expressed on these maximal figures. The 13-point cluster is a central site surrounded by its 12 nearest neighbors. The 14-point cluster is the standard fcc cube.

$$\Delta E^s_{\text{form}} = E^s - [c_A E^0_A + (1-c_A) E^0_B] \,, \tag{6.1}$$

where the superscript 0 indicates a pure element. Thus, if $\Delta E^s_{\text{form}} > 0$, then the concentration-weighted pure-element energies are lower than that of s, thus, the structure is unstable with respect to phase separation between pure A and pure B. Similarly, a negative value of ΔE^s_{form} implies that energetically, it is favorable (with respect to pure-element phase separation) for the alloy to order. Using Eqs. (4.3) and (6.1), the formation energy per lattice site may be written in terms of the ECI's and the cluster functions of $s, \bar{\sigma}^s_\alpha$, as [using the identity $c_A = (1+\bar{\sigma}_1)/2$]

$$\Delta E^s_{\text{form}} = \sum_{\Omega_L(\alpha)}^{\Omega_L(\alpha_m)} V_\alpha m_\alpha (\bar{\sigma}^s_\alpha - \Lambda_{n_\alpha}) \,, \tag{6.2}$$

with

TABLE VII. Ground-state superstructures of the fcc lattice. The structures are listed and discussed in the text first by their Strukturbericht designation. If none exists, then the prototype is used to distinguish different ordered phases. If neither Strukturbericht nor experimentally observed prototype exists, then an alternate labeling scheme is used, as in the $W1$ and $W8$ structures. Also given are the space group of the structure, its Pearson symbol, and references which describe the structure in detail.

Strukturbericht designation	Prototype	Space group	Pearson symbol	References
$L1_0$	AuCu	$P4/mmm$	$tP4$	Ref. 47
$L1_2$	$AuCu_3$	$Pm\bar{3}m$	$cP4$	Ref. 47
$D0_{22}$	Al_3Ti	$I4/mmm$	$tI8$	Ref. 47
	$MoPt_2$	$Immm$	$oI6$	Ref. 31
$D1_a$	Ni_4Mo	$I4/m$	$tI10$	Ref. 47
	Pt_8Ti, Ni_8Nb	$I4/mmm$	$tI18$	Ref. 33
	Ga_2Zr	$Cmmm$	$oC12$	This work
$W1$[a]	A_5B_3	$P4/mmm$	$tP8$	This work
$W8$[a], "Phase 13"[a]	A_5B (Ga_2Zr)	$Cmmm$	$oC12$	Ref. 31 and this work

[a]Not Strukturbericht designations. These symbols do not exist for these structures. The $W1$ and $W8$ structures are shown in Figs. 3(a) and 4. "Phase 13" refers to the numbering system of Kanamori and Kakehashi.

$$\Lambda_{n_\alpha} = \begin{cases} 1; & \text{for } n_\alpha \text{ even} \\ \bar{\sigma}_1; & \text{for } n_\alpha \text{ odd} \end{cases} \tag{6.3}$$

where n_α is the number of points in the cluster α. The two terms with $n_\alpha = 0, 1$ do not contribute to the formation energy as the orbit averages associated with these interactions are always 1 and $\bar{\sigma}_1$, respectively. Once the ECI's are computed for an alloy system, the energy of any structure (ordered or disordered) is trivially obtained from a knowledge of its orbit-averaged cluster functions. It is important to note that computing the formation energies from Eq. (6.2) is equivalent to computing the energies of each of the terms in Eq. (6.1) at the same volume [the volume at which the ECI's are calculated, given by Eq. (5.1) with $c = \frac{1}{2}$]. Thus, the energies computed from Eq. (6.2) will be termed *unrelaxed* formation energies because the pure-element reference points are not relaxed with respect to overall volume change.

The results of the ground-state searches for all of the six alloy systems are given in Figs. 2(a)–2(f). In each panel, the unrelaxed formation energies are plotted as a function of alloy composition. The ground states are designated by filled circles and in certain cases, metastable states which are energetically extremely competitive with the stable phases are plotted as open circles. The stable structures must lie on a convex hull; any concave region would imply that the structure is not stable with respect to phase separation between two other phases. The convex hull connecting the ground states is denoted by solid line in each of Figs. 2(a)–2(f). Also, for comparison, the energy of the completely disordered state on the fcc lattice is given in each figure as a dashed line. In the completely disordered state, the cluster functions reduce to products of the orbit-averaged point cluster function (linearly related to the concentration), and the formation energy of the disordered state is then easily computed from Eq. (6.2). The differences between the energy of a given ordered phase and that of the completely random state at the same concentration is sometimes referred to as the ordering energy, and provides a quantitative estimate of the relevant energy difference involved in an order-disorder transition. If this ordering energy is small for a particular phase, the phase will likely disorder at lower temperatures, and thus may not be observed experimentally. A large value of the ordering energy implies that the phase will be strongly ordered, hence will only disorder at high temperatures.

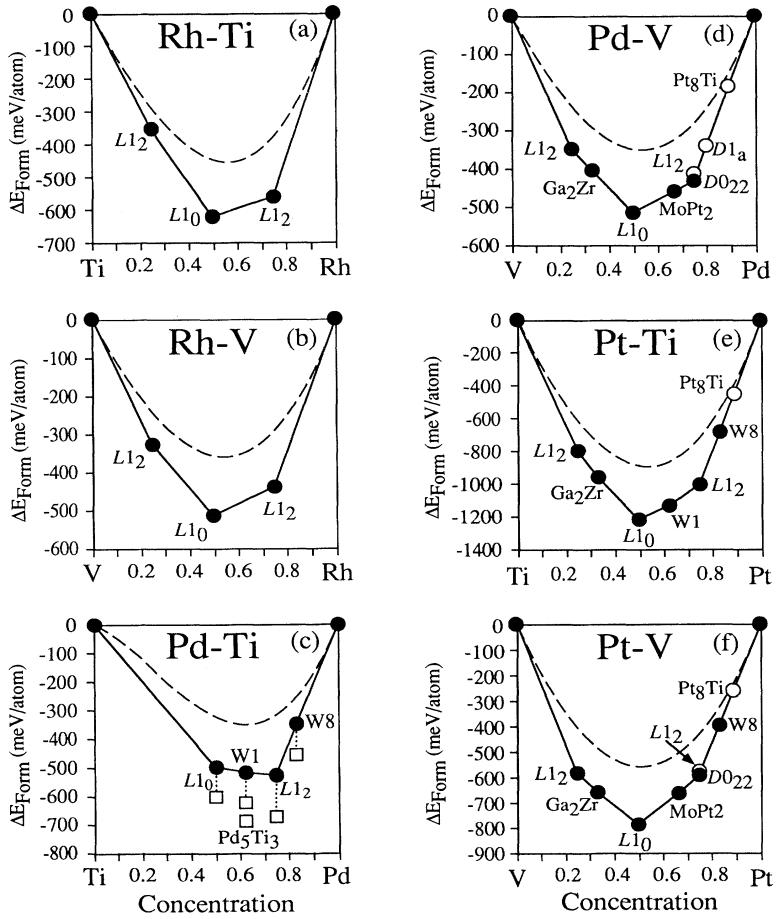

FIG. 2. Formation energies of the theoretically predicted fcc ground states in (a) Rh-Ti, (b) Rh-V, (c) Pd-Ti, (d) Pd-V, (e) Pt-Ti, and (f) Pt-V. Ground states are indicated by filled circles, and the convex hull connecting the stable structures is given by a solid line. The formation energy of the completely disordered state is indicated by a dashed line. Empty circles indicate metastable phases. For Pd-Ti, open squares indicate unrelaxed formation energies of five ordered compounds in the Pd-Ti system as computed directly from the self-consistent total-energy LMTO-ASA calculations described in the text.

A. Rh-Ti

The results of the fcc ground-state search for Rh-Ti are shown in Fig. 2(a). Three ordered fcc superstructures are theoretically predicted to be stable for Rh-Ti. For $c_{Rh} < 0.5$ we find the $L1_2$ structure (at composition $RhTi_3$). At compositions RhTi and Rh_3Ti, we find the $L1_0$ and $L1_2$ structures, respectively.

The experimental data for Rh-Ti has been compiled up to 1975 by Murray.[53] In all six alloy systems, only the experimentally observed fcc superstructures will be considered in detail, as these are the only data that can be compared with the predictions of the theory. Two fcc superstructures are experimentally observed in the Rh-Ti system. The low-temperature equiatomic phase is the fcc-based $L1_0$, in agreement with the theoretical predictions. Also, the $L1_2$ (Rh_3Ti) structure is observed experimentally, in agreement with the results of Fig. 2(a).

B. Rh-V

The predicted fcc ground states of Rh-V are shown in Fig. 2(b). The same ground-state structures are derived for this system as for Rh-Ti: an $L1_0$ at RhV, and two $L1_2$ structures at Rh_3V and RhV_3. A compilation of the experimental results up to 1977 is given by Smith.[54] The Rh-V system crystallizes into six intermediate phases, two of which are fcc-based: An off-stoichiometric tetragonal structure is observed at RhV and has been identified as $L1_0$, and a Rh_3V structure is observed with the $L1_2$ type of ordering. These two structures are both correctly predicted by the ground-state search.

C. Pd-Ti

The results of the ground-state search for Pd-Ti are shown in Fig. 2(c). Pd-Ti is interesting from the standpoint of its ECI's because of the relatively large triplet interactions present: The triplet $V_{3,1}$ is larger than any of the other interactions in the system, except $V_{2,1}$. The large triplet interactions in Pd-Ti tend to contribute large positive terms to the energy of the Ti-rich alloys and hence, translate into formation energies which are strongly asymmetric about $c_{Pd} = \frac{1}{2}$. The effects of the triplet interactions are evidenced by the fact that no intermediate fcc phases are predicted to be stable with respect to phase separation between $L1_0$ (the PdTi ground state) and pure Ti. At Pd_3Ti_2, a ground state is found, however, this phase has been proven to be inconstructible. Thus, we leave this inconstructible structure out of the ground-state diagram. (Simply omitting the structure from the ground-state convex hull could prove to be dangerous were the inconstructible vertex found to have an energy far below the closest competing tie line: In that case, another constructible structure with a slightly higher energy might be stable with respect to phase separation between two other compounds. However, in the case of Pd_3Ti_2, the inconstructible vertex was only stable with respect to phase separation between PdTi and Pd_5Ti_3 by 1.1 meV.) At Pd_5Ti_3, a new phase labeled $W1$ is predicted. The $W1$ phase is new in the sense that it has not been predicted in any previous ground-state search, and thus must only be stabilized when fourth-NN pairs and multiplet interactions are included in the energy expansion. The structure $W1$ is shown in Fig. 3(a). It is a simple tetragonal structure with space group $P4/mmm$, and eight atoms in the unit cell. A Pd_3Ti phase is found to have the structure of $L1_2$.

Also, a Pd_5Ti phase is predicted to be stable and is labeled $W8$. Because $W8$ has also been identified in the ground-state search of Kanamori and Kakehashi as number 13, we additionally label this compound as Phase 13, which has a prototype of Ga_2Zr. It is a base-centered orthorhombic compound with space group $Cmmm$ and 12 atoms per conventional unit cell. The $W8$ structure has four distinct Wyckoff positions and thus in general may be considered as a quaternary phase. By rearranging the atoms of a binary compound on Wyckoff positions with differing multiplicities, it is possible to obtain an A_5B phase with A_2B prototype. The $W8$ structure is shown in Fig. 4. The four types of symbols (filled and open circles, filled and open squares) indicate the symmetrically distinct sites. If Zr and Ga atoms are placed as follows: open circle—Ga_1, filled square—Ga_2, filled circle—Zr, open square—Ga_3, then the Ga_2Zr compound results. To obtain the (Pd_5Ti) $W8$ or Phase 13 structure, the sites are decorated in the following way: open circle—Pd_1, filled square—Ti, filled circle—Pd_2, open square—Pd_3. Thus, although these structures are symmetrically equivalent, the orbit averaged cluster functions which describe them are, of course, quite different. In light of these symmetry arguments, it is interesting to note that the results of Kanamori and Kakehashi include the $W8$

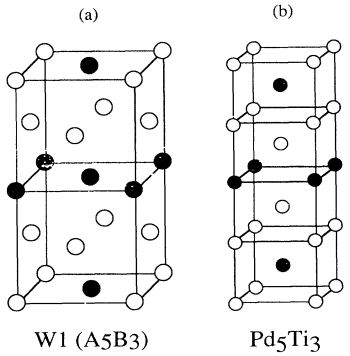

FIG. 3. (a) The $W1$ structure and (b) the experimentally observed Pd_5Ti_3 ground state. The $W1$ phase is predicted to be the lowest-energy fcc-based superstructure at Pd_5Ti_3 composition. This tetragonal phase has the $P4/mmm$ space group and eight atoms in the conventional unit cell. The experimentally observed Pd_5Ti_3 ground state is a bcc-based tetragonal structure which also is $P4/mmm$ with eight atoms in the unit cell.

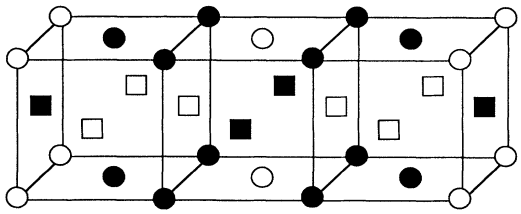

FIG. 4. The Ga_2Zr structure. This orthorhombic structure has a space group *Cmmm* and Pearson symbol *oC*12. The conventional unit cell has 12 atoms, four of which are distinct by symmetry. These four types of atoms (and their multiplicities) are given by open circles (2), filled circles (4), open squares (4), and filled squares (2). If the sites are decorated with Ga and Zr in the following manner: open circles—Ga_1, filled circles—Zr, open squares Ga_3, filled squares—Ga_2, then the Ga_2Zr structure results. If the decoration is given by open circles—Pd_1, filled circles—Pd_2, open squares—Pd_3, and filled squares—Ti, then the Pd_5Ti structure found in the ground-state analysis results. This structure is termed the *W*8 structure, or "Phase 13".

or Phase 13 structure, but not the Ga_2Zr phase, which is in fact, the prototype.

Experimentally, Pd-Ti has been studied extensively, however, there is very little agreement among the investigators about any feature of the system. Murray[53] has compiled the experimental results on Pd-Ti up to 1981. At equiatomic composition, PdTi transforms from a high-temperature *B*2 (bcc-based) compound into a low-temperature *B*19 (hcp-based) phase. Within two close-packed planes, *B*19 is equivalent to the $L1_0$ fcc-based structure, the type of ordering predicted by our calculations. There is also agreement about the existence of a compound slightly off Pd_3Ti stoichiometry which is the $L1_2$ structure. In addition, there is evidence[55] for a Pd_5Ti_3 structure, which has been described as a variant of the $MoSi_2$ or $C11_b$ (bcc-based) structure. However, this Pd_5Ti_3 phase appears to be a distinct, stoichiometric phase. Krautwasser *et al.*[56] have identified the crystal structure of the Pd_5Ti_3 phase. Both the space group (*P*4/*mmm*) and Pearson symbol (*tP*8) are identical with the *W*1 structure predicted by the theory. For comparison, the experimentally observed structure is also shown in Fig. 3(b) alongside *W*1.

Self-consistent, total-energy LMTO-ASA calculations have been performed on seven phases in the Pd-Ti system: Pure Ti, $L1_0$, *W*1 (Pd_5Ti_3), the experimentally observed Pd_5Ti_3 structure, $L1_2$ (Pd_3Ti), *W*8 (Pd_5Ti) and Pure Pd. The computations for the ordered compounds were performed as described above for the case of the pure elements. The total energies of all the phases were computed at the alloy lattice constant of the DCA calculations so that a direct comparison may be made between the formation energies obtained from fully self-consistent total energies of the LMTO-ASA and those predicted by the DCA (also the LMTO input, but neglecting the electrostatic terms of the total energy). The unrelaxed formation energies as calculated from the LMTO-ASA are shown in Fig. 2(c) as open squares, connected by dotted lines to the calculations of the DCA. The magnitudes of the total-energy formation energies in Fig. 2(c) are all slightly more negative than those calculated from the DCA computations. This discrepancy must be due to the neglect of electrostatic terms in the DCA results. The large asymmetry in formation energies about equiatomic concentration is evident in the DCA computations due to the large multiplet interactions, and is confirmed by the results of the LMTO calculations. Thus, the large triplet interactions in Pd-Ti obtained from the DCA are physically relevant and *must* be included in a cluster expansion of Pd-Ti energetics to accurately describe this system. The experimentally observed bcc-based Pd_5Ti_3 phase is calculated to have a lower formation energy (696 meV/atom) than that of the fcc-based *W*1 phase (628 meV/atom), which was predicted by the fcc ground-state search. The LMTO total-energy calculations also correctly place the formation energy of the experimentally observed phase below the tie line connecting the $L1_0$ and $L1_2$ phases, while the energy of the unrelaxed *W*1 structure lies slightly above this line. Also, the results of the total energy LMTO-ASA calculations show the energy of the unrelaxed *W*8 structure to lie slightly below the tie line between $L1_2$ and pure Pd, in agreement with the DCA computations.

D. Pd-V

The results of the fcc ground-state search for Pd-V are presented in Fig. 2(d). For $c_{Pd} < 0.5$ we have found the $L1_2$ (PdV_3) structure and the Ga_2Zr (PdV_2) as stable phases. The Ga_2Zr structure has not been predicted in any previous ground-state analyses, and thus must be stabilized only by including fourth-NN pairs and multiplet interactions in the energy expansion. Additionally, because Kanamori and Kakehashi[31] did not find the Ga_2Zr structure in their ground-state search with pairs alone, we may conclude that Ga_2Zr is stabilized by multiplet interactions. At PdV, Pd_2V, and Pd_3V compositions, we find $L1_0$, $MoPt_2$-type, and $D0_{22}$ to be the stable structures, respectively. For $c_{Pd} > 0.75$ the ordered structures, $D1_a$ and Pt_8Ti-type, are virtually on the tie line between $D0_{22}$ and pure Pd, so that we cannot draw any definite conclusions, except that both structures will at least be energetically competitive with other phases. The ordering energy of the Pt_8Ti-type phase is quite small (32 meV$=k_B \times 370$ K) so that even were this phase stable, kinetics might prevent it from being experimentally observed as it is likely that the phase would disorder at low temperatures. The slight numerical discrepancies between the results of Fig. 2(d) and those of Ref. 57 are due to small convergence errors in the LMTO *k*-point sampling used in the previous calculations. While the values of some formation energies are slightly altered, the ground states of order are identical. As described in Ref. 57, the results of the ground-state search for fcc Pd-V alloys are in excellent agreement with experimental observations.

E. Pt-Ti

The calculated fcc ground states for Pt-Ti are shown in Fig. 2(e). There are six intermediate constructible fcc superstructures identified as ground states in this system. For $c_{Pt} < 0.5$, two structures are predicted: an $L1_2$ structure at stoichiometry $PiTi_3$ and a $PtTi_2$ compound isostructural with Ga_2Zr. The $L1_0$ structure is predicted to be the stable equiatomic structure, and $W1$ is again identified as the Pt_5Ti_3 phase. $L1_2$ (Pt_3Ti) and the $W8$ (Pt_5Ti) structure are found as ground states. Both $W8$ and Pt_8Ti are virtually on the tie line between $L1_2$ and pure Pt, so the precise stability or metastability of these phases cannot be determined. The $W8$ phase is 12 meV below the tie line between $L1_2$ and pure Pt; however, the Pt_8Ti phase is only 3 meV above the tie line between $W8$ and pure Pt, and actually 5 meV below the tie line between $L1_2$ and Pt. Thus, were it not for the existence of the $W8$ phase, Pt_8Ti would be a ground state in this calculation. Also, the same inconstructible vertex stabilized in Pd-Ti is found here at Pt_3Ti_2.

The experimental data for Pt-Ti up to 1981 have been compiled by Murray.[53] As in the Rh-Ti and Pd-Ti alloys, Ti-rich compounds are not fcc based. As is the case for Pd-Ti, there is a high-temperature equiatomic $B2$ phase which transforms martensitically to a low-temperature $B19$ structure that is closely related to the fcc-based $L1_0$ structure, the ground state predicted at this composition. An orthorhombic Pt_5Ti_3 structure is observed, but its absolute stability at low temperatures is still uncertain. The $L1_2$ phase is also observed at stoichiometry Pt_3Ti, as predicted by our calculations. The existence of a Pt_8Ti phase has been reported[58,59] and has a tetragonal structure isostructural with Ni_8Nb. This structure is calculated to be only unstable by 3 meV/atom, an amount certainly well within the theoretical uncertainty. Additionally, fcc-based long-period superstructures (LPS) have been found in this system[59] between the Pt_3Ti and Pt_8Ti stoichiometries, which incorporate features of the $L12$ and Pt_8Ti structures, however, whether or not these structures are true ground states or stabilized only at elevated temperatures is still unanswered. Also, incorporating LPS such as these in a theoretical ground-state analysis would presumably require ECI's which extend outside the fourth-NN range.

In addition, the magnitude of the heats of formation may be compared directly with experimental investigations. The results of Fig. 2(e) may be compared with calorimetric data,[60] which have been reported for the Pt-Ti system; however, it must be kept in mind that Fig. 2(e) contains unrelaxed formation energies. That is, the pure-element energies in Eq. (6.1) are effectively at the alloy volume, and not their equilibrium volume. Relaxing the pure elements to their equilibrium volumes will tend to add positive terms to the strained formation energy. Thus, the strained formation energies are always more negative than the actual heats of formation. The experimental results for Pt_3Ti ($L1_2$) and Pt_8Ti are -0.970 eV/atom and -0.407 eV/atom, respectively. The calculated numbers are -1.00 eV/atom and -0.45 eV/atom for $L1_2$ and Pt_8Ti, respectively, in reasonable accord with the experimental results.

F. Pt-V

The results of the fcc ground-state search in Pt-V are shown in Fig. 2(f). In V-rich alloys, the $L1_2$ and Ga_2Zr structures are predicted, with stoichiometries, PtV_3 and PtV_2. $L1_0$ is predicted to be the lowest-energy structure at equiatomic composition. The Pt_2V and Pt_3V structures are $MoPt_2$ and $D0_{22}$, respectively. The $L1_2$ phase at Pt_3V stoichiometry is very competitive with the $D0_{22}$, with the energy difference between these two structures being just 7 meV/atom. Just as in Pt-Ti, the $W8$ and Pt_8Ti structures are virtually on the tie line between the Pt_3V compound and pure Pt: The $W8$ is less than 1 meV/atom below the Pt_3V-Pt tie line, and Pt_8V is less than 1 meV/atom above this line. Thus, the (meta)stability of these phases are uncertain in these calculations. Another similarity with the Pt-Ti system is the existence of the inconstructible Pt_3Ti_2, again predicted here.

The experimental investigations of Pt-V are summarized by Smith[54] and Schryvers and Amelinckx.[61] There is a general agreement that at least four intermediate phases occur with stoichiometries PtV_3, PtV, Pt_2V, and Pt_3V. The PtV_3 structure is isostructural with Cr_3Si ($A15$), and is not an fcc-based compound. The PtV structure is the $B19$ phase, which is consistent with the $L1_0$-type ordering predicted here. The Pt_2V and Pt_3V phases are the $MoPt_2$ and $D0_{22}$ structures, just as predicted by the ground-state search. In addition, there is evidence[61,62] of a tetragonal Pt_8V structure (of Pt_8Ti-type), analogous to Ni_8V.

Several reports of metastable and high-temperature phases also indicate the accuracy of the DCA calculations: Studies of Pt-V alloys near the Pt_3V composition have shown evidence of the $L1_2$ type of ordering, but the experimental evidence indicates that this $AuCu_3$-type phase is likely to be slightly metastable, as predicted by our calculations. However, at temperatures near 1000 °C, the existence of fcc-based LPS has been reported at Pt_3V stoichiometry.[61,63] These LPS are formed by periodically shifting cells of an $L1_2$ structure with respect to each other (or creating an antiphase boundary) by the vector $1/2[110]$. The structure then may be specified by the mean number of $L1_2$ cells between antiphase boundaries, denoted by M. The minimum of $M=1$ results in the $D0_{22}$ structure, while the maximum ($M=\infty$) denotes the $L1_2$ phase. The $M=4/3$ structure has been observed in Pt_3V, and computing the energy of this LPS with the Pt-V ECI's given in Table IV places the energy of the $M=4/3$ structure between that of the $D0_{22}$ and $L1_2$, and only 2-meV higher than the $D0_{22}$ ground state. Thus, there is clearly a close competition for stability between the $D0_{22}$ and the LPS. Additionally, the existence of $L1_0$ ordering in equiatomic PtV alloys has been reported,[56,64] however, this structure appears to be metastable. Also, $L1_2$-type ordering at PtV_3 compositions has been reported in coexistence with the Cr_3Si-type structure,[56] howev-

er, there is agreement that the existence of the $L1_2$ is due to contamination from interstitial elements, such as oxygen and possibly nitrogen and/or carbon.

VII. DISCUSSIONS AND CONCLUSIONS

The combination of the energy expansion in an Ising-like framework and an *ab initio* technique for computing the ECI's leads to a first-principles Ising model of alloy energetics. The energy expansion in terms of concentration-independent ECI's is exact in the sense that the basis functions are orthonormal and complete in the space of all possible configurations and in the present paper, we have seen the advantages of using such an expansion. The computation of the ECI's is crucial in an Ising model approach: The ECI's provide an extremely convenient parametrization of the energy with respect to substitutional variations of atoms on a fixed lattice and are hence, the building blocks of the energetic description of the alloy. The method of DCA has been used in this paper to compute the ECI's. The idea behind the DCA is simply to compute the ECI's as closely as possible from the exact definition given by the inner product of the appropriate cluster function with the energy. However, the definition of the ECI's involves averaging over configurations which are not translationally invariant, and thus, necessitates a real-space technique for diagonalizing the Hamiltonian. DCA is based entirely in real space, thus making the calculation of properties of the disordered systems conceptually no more difficult than that of the ordered states. Additionally, this direct method provides a non-mean-field description of the completely disordered state, unlike the site-only coherent-potential approximation (S-CPA). With this distinction in mind, however, comparisons[65] between the DCA and the cluster extensions of the CPA (e.g., the generalized perturbation method[66] and embedded-cluster method[67]) indicate a remarkable similarity between the two techniques for both pair and multiplet interactions computed for simple model systems. The DCA is currently realizable within the context of a TB-LMTO Hamiltonian, and the real-space nature of the DCA also makes the method extremely flexible in dealing with systems of broken topological symmetry: The DCA has already been used to study surfaces and interfaces,[68,69] and many encouraging results have been obtained.

The self-consistency used in the DCA calculations is based upon making each configurationally averaged atom locally neutral. This scheme of configurationally averaged neutrality was checked against the results of fully self-consistent LMTO-ASA calculations on ordered compounds. The d-band on-site energies of fcc Pd-V and Pt-V alloys were in excellent agreement with the LMTO-ASA results, and the discrepancy in the s and p bands was seen to lead to negligible errors in the ECI's for the Pd-V system. The deepening of the Pt s band due to scalar relativistic corrections was seen to enhance the ordering trends in Pt-V relative to that of Pd-V.

A large set of ECI's on the fcc lattice were calculated for each of the six transition-metal alloys formed by the combination of Rh, Pd, and Pt with Ti and V: Rh-Ti, Rh-V, Pd-Ti, Pd-V, Pt-Ti, and Pt-V. Due to d-band tight-binding arguments, it is expected that all these systems should strongly order. This prediction is supported by experimental evidence, and is also consistent with the dominant, positive value of the nearest-neighbor pair interaction computed in all six cases. The convergence of the energy expansion with respect to its coefficients was seen to be fairly rapid, provided that fourth-NN pair and several triplet and quadruplet interactions were included. The multiplets are crucial to obtaining the experimentally observed ground states in the transition-metal alloys considered here, and in some cases, they are even responsible for stabilizing new ground states, i.e., structures that would not be stabilized with only pair interactions. Thus, it is clear that multiplet ECI's simply may not be neglected in the energy expansion.

Given a set of ECI's for a fixed lattice, it is possible to solve exactly for the minimum energy configurations on this lattice, as a function of concentration. This ground-state analysis is contingent upon minimizing the cluster expansion of the energy, subject to a number of geometrical constraints, which have been formulated on the (13–14)-point clusters using group theoretic arguments. These constraints, along with the energy expansion were used to solve for the fcc ground-state structure of all six alloys. In all cases, the results of this combined quantum- and statistical-mechanical approach were in excellent agreement with the experimental results for fcc-based structures: In no case was an unambiguously experimentally determined fcc-based phase missing from the results of the ground-state search. The extension of this ground-state search to other underlying lattices should be pursued, as many common alloy intermetallics are superstructures of not only fcc, but bcc and hcp as well. These extensions should certainly be tractable in the case of bcc, and also in hcp, although the symmetry of the hcp lattice is such that for a given range of interactions, certain clusters which are equivalent in the fcc problem become nonequivalent, and thus, complicate the issue. Many intermetallic systems, such as the ones considered in this paper, also contain complex structures, which are not based on any of the common elemental structures. These complex structures are not directly amenable to the type of ground-state search outlined here, which will only predict the lowest-energy superstructures of a given parent lattice. In addition, long-period superstructures can, in principle, be detected by a real-space ground-state search, but for example, the long-period structures based on the $L1_2$ structure (as found in Pt-V) would presumably be stabilized by a set of interactions whose range was beyond that of fourth-NN, which would make the calculation of constraints extremely cumbersome, if not impossible.

In sum then, the energy expansion in terms of concentration-independent ECI's is seen to provide a valid description of the energetics of alloy systems. Even in cases where the formation energies are strongly asymmetric about $c=0.5$, these asymmetries are accurately represented by inclusion of multiplet terms in the expansion of the energy. In addition to the validity of this expansion, we have seen its practicality in facilitating the

ground-state search. Also, DCA has been used in the past[2,17] to predict general qualitative trends in alloy systems. However, we have shown here interactions computed from DCA with no adjustable parameters may be used as a quantitative tool in the study of alloy phase stability. And finally, an exact ground-state search for real alloy systems has been performed for the fcc lattice including pairs up to fourth NN and multiplets. This technique has lead to results which are in excellent agreement with experiment for six transition-metal alloys.

ACKNOWLEDGMENTS

This work was supported by the Office of Energy Research, Office of Basic Energy Sciences, Materials Sciences Division of the U.S. Department of Energy under Contract No. DE-AC03-76SF00098, and by grants from NATO (No. 0512/88) and from the National Science Foundation (No. INT-8815493). One of the authors (D.d.F.) would like to acknowledge the support of the Advanced Materials and Technology Research Laboratories of the Nippon Steel Corporation. The authors wish to thank Professor Leo Falicov, Mark Asta, and Dr. Prabhakar Singh for many helpful discussions, and Dr. Mark van Schilfgaarde for generously making available to them an LMTO-ASA code.

APPENDIX

We present here a discussion of the convergence properties of (1) the ECI's with respect to configurational averaging, and (2) the cluster expansion itself with respect to the number of terms retained. The set of ECI's calculated from Eqs. (2.10) and (2.11) for the Pd-V system are given in Table III. Of course, the configurational averaging involved in the definition of the ECI's (e.g., $V_{pp'}=\{\Delta_2 E\}$) is, in principle, over all the configurations of the entire system. However, for practical purposes, this averaging is only done over a small number of configurations, $N_{\rm conf}$. Thus, in practice the curly brackets, $\{\cdots\}$, represent an average over $N_{\rm conf}$ configurations, which are selected at random from the total possible 2^{N-n_α} configurations, where $n_\alpha=2$ for pairs, 3 for triplets, etc. It is important to note that each of these 2^{N-n_α} configurations has an *equal probability* of being selected. There is no inherent bias in the selection process. Thus, in the computation of the ECI's, $\Delta_{n_\alpha}E(\sigma)$ is computed for each of the $N_{\rm conf}$ configurations, and the average gives $V_{p\ldots p'}=\{\Delta_{n_\alpha}E(\sigma)\}$. There is also a standard deviation associated with this list of values of $\Delta_{n_\alpha}E(\sigma)$ which may be tabulated as

$$\Sigma_{\rm conf}=\sqrt{\{(\Delta_{n_\alpha}E(\sigma)-V_{p\ldots p'})^2\}}\ . \tag{A1}$$

It is well known from statistics that if a set of $N_{\rm conf}$ data points has a deviation of $\sigma_{\rm conf}$, then the deviation of the mean of the set is simply $\Sigma_{\rm conf}/(N_{\rm conf})^{1/2}$. Thus, this deviation of the mean gives a quantitative estimate of the error induced in the ECI's by only considering a finite number of configurations. These values are also listed in Table III along with the values of $N_{\rm conf}$ used for each computation.

From Table III, we see that the cluster expansion is rapidly convergent with respect to the ECI's considered, provided that multiplet (interactions with clusters larger than pairs) interactions are included. The NN pair interaction is dominant and positive, which indicates a strongly ordering system. The pair interactions rapidly decay as the distance increases between the pairs, but even up to 3rd or 4th NN pairs, they could not be termed negligible. (A note of explanation is in order here: Interactions are given to an accuracy of 0.1 meV, which is clearly below the accuracy of the LDA, and hence the LMTO Hamiltonian used to generate these interactions. However, what must be considered is the contribution that these ECI's make to the energy expansion: It is really the interaction times its multiplicity which is relevant. For example, in the case of Pd-V, the 2nd and 3rd NN pairs actually contribute a comparable amount to the configurational energy as the 2nd NN pair has a multiplicity of 3 whereas the 3rd NN is multiplied by a factor of 12.) The triplet interactions are also quite large, especially $V_{3,1}$, which is composed of three NN bonds (the most compact triangle possible on the fcc lattice), and $V_{3,4}$ which is a straight line of three points along the (110) direction. Some previous tight-binding arguments[48,70] have indicated that clusters composed of self-retracing straight paths should be important, but these arguments also indicate the relative unimportance of multiplet interactions composed of compact clusters. Additional arguments[71] have been made asserting the importance of compact clusters over the straight line clusters. However, what we see here is that actually *both* are critical to obtain a convergent expansion. The quadruplet interactions are quite small in comparison with the triplets and pairs, indicating again the rapid convergence of the expansion. The most compact cluster, the fcc tetrahedron $V_{4,1}$, gives the largest quadruplet interaction, while the straight line path $V_{4,3}$ is quite small. Many of the 27 interactions computed for this system are completely negligible, however, it is necessary to perform these calculations to verify the convergence.

The pair interactions are averaged over 50 configurations, which leads to an accuracy of between 2% (for 2nd NN pair) and 25% (for 4th NN pair). In addition, these errors induced by considering $N_{\rm conf}\ll 2^{N-n_\alpha}$ are all below 1 meV with the exception of the NN pair. The triplet interactions are averaged over a significantly smaller set of configurations (15–30), however, the relative errors are even smaller (the errors range from 1 to 20%), which indicates that the quantity $\Delta_3 E(\sigma)$ is much less sensitive to variations of the local environment than is $\Delta_2 E(\sigma)$. Correspondingly, the quadruplet interactions are averaged over an even smaller set of configurations, but their errors are completely negligible (0.3–2%). Therefore, as the number of points in the cluster increases, the dependence of the ECI on the medium outside the cluster decreases. One could average quadruplet interactions over a mere five configurations and still maintain a high degree of accuracy.

In addition, these error values lead to an interesting criterion for determining the degree of convergence of

the expansion. In Ref. 4, two distinct schemes of averaging were shown to lead to equivalent expansions. In one expansion [that of Eq. (2.6)], the interactions are coefficients of cluster functions, which are orthonormal with respect to the trace over all configurations of the system. These ECI's are then configuration independent, and hence concentration independent. In an alternate scheme, the defining trace may be made only over all configurations of the system which are consistent with a given concentration leading to ECI's which are concentration dependent. A relationship was derived between these two sets of ECI's which essentially showed the following: The concentration-independent ECI's were equivalent to the concentration-dependent ECI's which were renormalized by higher-order cluster interactions. For example, if the NN pair interaction is strongly concentration dependent, there must exist other multiplet interactions (which contain the NN pair as a subcluster) which are of sizeable magnitude. From Table III, we can see that this criterion may be put into practice in determining, at least qualitatively, the level of convergence: If the value $\Delta_2 E(\sigma)$, for a certain pair p,p', is strongly configuration dependent, there will be a large degree of deviation from the mean value of $V_{pp'}$. Correspondingly, the error for $V_{pp'}$ will be large. A strong configuration dependence of $\Delta_2 E(\sigma)$ also necessarily implies that there be a large degree of concentration dependence of the quantity $\{\Delta_2 E(\sigma)\}_c$, where the curly brackets $\{\cdots\}_c$ denote averaging with respect to all configurations consistent with a given concentration, c. The quantity $\{\Delta_2 E(\sigma)\}_c$ is simply the effective pair interaction in the concentration-dependent averaging scheme.[3,4] Thus, the strong *configuration* dependence of $\Delta_2 E(\sigma)$, or, equivalently, a large value of Σ_{conf} implies that there must be at least one significant multiplet interaction which contains pp' as a subcluster. In the Pd-V case, we see that $V_{2,1}$ and $V_{2,4}$ both have a significant error associated with the average over 50 configurations, which implies that there must be significant triplet interactions containing first and fourth NN pairs as subclusters. The triplet $V_{3,1}$, which contains three NN pairs as subclusters, is indeed the largest triplet interaction. Also, $V_{3,4}$ (two NN bonds and one 4th NN bond) is large, although not quite as large as the error for the 4th NN pair is not as large as it is for $V_{2,1}$. The only triplet with a sizable error is the NN triangle, and the tetrahedron which contains four NN triangles as subclusters is the largest quadruplet interaction. Because the quadruplet interactions all have a negligible error associated with their configurational average, this implies that there are no significant higher-order terms with these quadruplets as subclusters. Therefore, at this stage, we may say with some confidence that the expansion is converged with this set of interactions.

Convergence of the expansion is critical to its usefulness, therefore, a thorough investigation of the convergence properties of the interactions has been presented here. It is seen in the Pd-V system how the criterion of Ref. 4 may be put into practice in determining which interactions will be non-negligible for a given system. Although these results have been derived from a tight-binding Hamiltonian, these general trends are likely to be valid regardless of the Hamiltonian used. If anything, the short-range tight-binding Hamiltonian could indicate a *faster* convergence of the energy expansion than would be obtained with long-range, more accurate Hamiltonians, particularly in nontransition metals.

[1] J. M. Sanchez, F. Ducastelle, and D. Gratias, Physica A **128**, 334 (1984).

[2] H. Dreyssé, A. Berera, L. T. Wille, and D. de Fontaine, Phys. Rev. B **39**, 2442 (1989).

[3] A. Gonis, X.-G. Zhang, A. J. Freeman, P. Turchi, G. M. Stocks, and D. M. Nicholson, Phys. Rev. B **36**, 4630 (1987).

[4] M. Asta, C. Wolverton, D. de Fontaine, and H. Dreyssé, Phys. Rev. B **44**, 4907 (1991).

[5] C. Wolverton, M. Asta, H. Dreyssé, and D. de Fontaine, Phys. Rev. B **44**, 4914 (1991).

[6] R. Kikuchi, Phys. Rev. **81**, 988 (1951); J. M. Sanchez and D. De Fontaine, Phys. Rev. B **21**, 216 (1980); **25**, 1759 (1982).

[7] K. Binder, Phys. Rev. Lett. **45**, 811 (1980); K. Binder, J. L. Lebowitz, M. K. Phani, and M. H. Kalos, Acta Metall. **29**, 1655 (1981); M. K. Phani, J. L. Lebowitz, and M. H. Kalos, Phys. Rev. B **21**, 4027 (1980).

[8] J. Van Der Rest, F. Gautier, and F. Brouers, J. Phys. F **5**, 2283 (1975); M. Cyrot and F. Cyrot-Lackmann, J. Phys. F **6**, 2257 (1976); D. G. Pettifor, Phys. Rev. Lett. **42**, 846 (1979); A. Bieber and F. Gautier, Acta Metall. **34**, 2291 (1986); M. Sluiter, P. Turchi, and D. de Fontaine, J. Phys. F **17**, 2163 (1987).

[9] Z. W. Lu, S.-H. Wei, and A. Zunger, Phys. Rev. Lett. **66**, 1753 (1991).

[10] V. Heine, Solid State Phys. **35**, 1 (1980).

[11] M. O. Robbins and L. M. Falicov, Phys. Rev. B **29**, 1333 (1984).

[12] M. van Schilfgaarde, A. T. Paxton, A. Pasturel, and M. Methfessel, in *Alloy Phase Stability and Design,* edited by G. M. Stocks, D. Pope, and A. Giamei, MRS Symposia Proceedings No. 186 (Materials Research Society, Pittsburgh, 1991).

[13] H. L. Skriver, Phys. Rev. B **31**, 1909 (1985).

[14] T. L. Einstein and J. R. Schrieffer, Phys. Rev. B **7**, 3629 (1973).

[15] N. R. Burke, Surf. Sci. **58**, 349 (1976).

[16] R. Haydock, Solid State Phys. **35**, 215 (1980).

[17] A. Berera, H. Dreyssé, L. T. Wille, and D. de Fontaine, J. Phys. F **18**, L49 (1988).

[18] J. Kanamori, Prog. Theor. Phys. **35**, 16 (1966).

[19] A. Finel and F. Ducastelle, in *Phase Transformations in Solids,* edited by T. Tsakalakos (North-Holland, Amsterdam, 1984), pp. 293–298.

[20] A. Finel, These de Doctorat d'Etat, Université de Paris VI, 1987.

[21] T. Kudo and S. Katsura, Prog. Theor. Phys. **56**, 435 (1976).

[22] J. Kanamori, J. Phys. Soc. Jpn. **53**, 250 (1984).

[23] A. K. Singh and S. Lele, Philos. Mag. B **65**, 967 (1982).

[24] A. K. Singh and S. Lele, Philos. Mag. B **64**, 275 (1991).

[25] A. K. Singh, V. Singh, and S. Lele, Acta Metall. Mater. **39**, 2847 (1991).

[26]F. Ducastelle, *Order and Phase Stability in Alloys* (North-Holland, New York, 1991).
[27]G. Inden and W. Pitsch, in *Materials Science and Technology,* edited by Peter Hassen (VCH, Weinheim, 1991), Vol. 5, pp. 497–552.
[28]M. J. Richards and J. W. Cahn, Acta Metall. **19**, 1263 (1971).
[29]S. M. Allen and J. W. Cahn, Acta Metall. **20**, 423 (1972); S. M. Allen and J. W. Cahn, Scr. Metall. **7**, 1261 (1973).
[30]J. M. Sanchez and D. de Fontaine, *Structure and Bonding in Crystals* (Academic, New York, 1981), Vol. II, p. 117.
[31]J. Kanamori and Y. Kakehashi, J. Phys. (Paris) Colloq. **38**, C7-274 (1977).
[32]P. Turchi, G. Stocks, W. Butler, D. Nicholson, and A. Gonis, Phys. Rev. B **37**, 5982 (1988).
[33]Z. W. Lu, S.-H. Wei, A. Zunger, S. Frotapessoa, and L. G. Ferreira, Phys. Rev. B **44**, 512 (1991).
[34]Z. W. Lu, S.-H. Wei, A. Zunger, and L. G. Ferreira, Solid State Commun. **78**, 583 (1991).
[35]G. Garbulsky and G. Ceder (private communication).
[36]J. M. Sanchez and D. de Fontaine, Phys. Rev. B **17**, 2926 (1978).
[37]V. Chvatal, *Linear Programming* (Freeman, New York, 1983); G. B. Dantzig, *Linear Programming and Extensions* (Princeton University Press, Princeton, NJ, 1963).
[38]P. Hohenberg and W. Kohn, Phys. Rev. B **136**, 864 (1964).
[39]W. Kohn and L. J. Sham, Phys. Rev. A **140**, 1133 (1965).
[40]O. K. Andersen, Phys. Rev. B **12**, 3060 (1975); O. K. Andersen, O. Jepsen, and D. Glotzel, in *Highlights of Condensed Matter Theory,* edited by F. Bassani *et al.* (North-Holland, Amsterdam, 1985).
[41]M. van Schilfgaarde (private communication).
[42]O. K. Andersen, Phys. Rev. B **12**, 3060 (1975); A. M. Bratkovsky and S. Y. Savrasov, J. Comp. Phys. **88**, 243 (1990).
[43]U. von Barth and L. Hedin, J. Phys. C **5**, 1629 (1972).
[44]O. K. Andersen and O. Jepsen, Phys. Rev. Lett. **53**, 2571 (1984); O. K. Andersen, O. Jepsen, and M. Sob, *Electronic Band Structure and Its Applications,* Lecture Notes in Physics Vol. 283, edited by M. Yussouf (Springer, Berlin, 1987).
[45]H. Shiba, Prog. Theor. Phys. **46**, 77 (1971).
[46]H. Dreyssé and R. Riedinger, J. Phys. (Paris) **48**, 915 (1987).
[47]D. de Fontaine, Solid State Phys. **34**, 73 (1979).
[48]F. Ducastelle, in *Alloy Phase Stability,* Vol. 163 of *NATO Advanced Study Institute, Series E: Advanced Sciences,* edited by G. M. Stocks and A. Gonis (Kluwer Academic, Boston, 1989).
[49]J. Friedel, in *The Physics of Metals,* edited by J. M. Ziman (Cambridge University Press, London, 1969).
[50]A. R. Miedema, R. Boom, and F. R. DeBoer, J. Less-Common Met. **41**, 283 (1975).
[51]C. D. Gelatt, A. R. Williams, and V. L. Moruzzi, Phys. Rev. B **27**, 2005 (1983).
[52]G. Ceder, Ph.D. thesis, University of California at Berkeley, 1991 (unpublished) available from University Microfilms International, Ann Arbor, MI, Order No. 9203517.
[53]J. L. Murray, in *Phase Diagrams of Binary Titanium Alloys* (ASM International, Metals Park, OH, 1987).
[54]J. F. Smith, in *Phase Digrams of Binary Vanadium Alloys* (ASM International, Metals Park, OH, 1987).
[55]E. Raub and E. Roeschel, Z. Metall. **59**, 112 (1968).
[56]P. Krautwasser, S. Bhan, and K. Schubert, Z. Metall. **59**, 724 (1968).
[57]C. Wolverton, G. Ceder, D. de Fontaine, and H. Dreyssé, Phys. Rev. B **45**, 13 105 (1992).
[58]P. Pietrokowsky, Nature (London) **206**, 291 (1965).
[59]D. Schryvers, J. van Landuyt, G. van Tendeloo, and S. Amelinckx, Phys. Status Solidi A **76**, 575 (1983).
[60]N. Selhaoui, Ph.D. thesis, Université de Nancy, France, 1990; P. J. Meschter and W. L. Worrell, Metall. Trans. **7A**, 299 (1976).
[61]D. Schryvers and S. Amelinckx, Acta Metall. **34**, 43 (1986).
[62]J. Planès, Thèse de Doctorat, Université Paris, 1990.
[63]J. Planès, A. Loiseau, F. Ducastelle, and G. van Tendeloo, *Electron Microscopy and Analysis 1987,* Proceedings of the Institute of Physics, No. 90, edited by M. L. Brown (Institute of Physics and Physical Society, London, 1987), p. 261.
[64]R. M. Waterstrat, Metall. Trans. **4**, 455 (1973).
[65]A. Berera, Phys. Rev. B **42**, 4311 (1990).
[66]F. Ducastelle and F. Gautier, J. Phys. F **6**, 2039 (1976).
[67]A. Gonis and J. W. Garland, Phys. Rev. B **16**, 2424 (1977).
[68]H. Dreyssé, G. Ceder, D. de Fontaine, and L. T. Wille, Vacuum **41**, 446 (1990).
[69]H. Dreyssé, L. T. Wille, and D. de Fontaine, Solid State Commun. **78**, 355 (1991).
[70]A. Bieber and F. Gautier, J. Phys. Soc. Jpn. **53**, 2061 (1984).
[71]M. Sluiter, D. de Fontaine, X. Q. Guo, R. Podloucky, and A. J. Freeman, Phys. Rev. B **42**, 10 460 (1990); J. W. D. Connolly and A. R. Williams, *ibid.* **27**, 5169 (1983).